Preparation of the polymer-bound SN-38 (SN-38 remaining bound to PEG-PGlu). To permit complete release of SN-38 from the conjugate, 20 μL of plasma and 100 μL of tissue samples were diluted with 20 μL of methanol (50%, v/v) and 20 μL of NaOH (0.3 mol/L for plasma and 0.7 mol/L for tissue). The samples were incubated for 15 minutes at 25°C. After incubation, 20 μL of HCl (0.3 mol/L for plasma and 0.7 mol/L for tissue) and 60 μL of internal standard solution were added to the samples, and then the hydrolysis was filtered through a MultiScreen Solvinert. The filtrate was applied to the high-performance liquid chromatography system.

High-performance liquid chromatography. Reversed-phase high-performance liquid chromatography was done at 35°C on a Mightysil RP-18 GP column 150 × 4.6 mm (Kanto Chemical Co., Inc., Tokyo, Japan). The samples were injected into an Alliance Waters 2795 high-performance liquid chromatography system (Waters, Milford, MA) equipped with a Waters 2475 multi λ fluorescence detector. The detector was set at 365 and 430 nm (excitation and emission, respectively) for CPT-11 and CPT, and at 365 and 540 nm for SN-38. A reversed-phase column was used at 35°C. The mobile phase was a mixture of 100 mmol/L ammonium acetate (pH 4.2) and methanol [11:9 (v/v) for SN-38 in plasma and tumor, 3:2 (v/v) for CPT-11 in plasma, and 63:37 (v/v) for CPT-11 in tumor]. The flow rate was 1.0 mL/min. Peak data were recorded with a chromatography management system (Empower, Waters). Polymer-bound SN-38 was determined by subtraction of polymer-unbound SN-38 from the total SN-38 of the hydrolysate.

Pharmacokinetic and Statistical Analyses

The concentrations of SN-38 and CPT-11 in plasma and tissue were fitted to a pharmacokinetic model by the nonlinear least-square method using WinNonlin Professional software (version 4.1; Pharsight Corp., Palo Alto, CA). We used a noncompartmental analysis. The pharmacokinetic variables were calculated using the following equations (AUC_{last} was calculated by the trapezoidal rule to the last measurable data point):

$$AUC_{inf.} = \int_0^{\infty} C(t)dt$$

$$T_{1/2z}(\text{terminal half} - \text{life}) = 0.693/\lambda z$$

(λz is first-order rate constant associated with the terminal portion of the curve)

$$CL_{tot} = \text{Dose}/AUC_{inf.}$$

$$V_{ss} = MRT \times CL_{tot}(\text{MRT, mean residence time})$$

Data were expressed as mean ± SD. Data were analyzed with the Student's t test when the groups showed equal variances (F test) or with Welch's test when they showed unequal variances (F test). $P < 0.05$ was regarded as statistically significant. All statistical tests were two sided.

Results

Preparation and characterization of NK012. NK012 is an SN-38-loaded polymeric micelle constructed in an aqueous milieu by the self-assembly of an amphiphilic block copolymers, PEG-PGlu(SN-38). The molecular weight of PEG-PGlu(SN-38) was determined to be ~19,000 (PEG segment, 12,000; SN-38-conjugated PGlu segment, 7,000). NK012 was obtained as a freeze-dried formulation and contained ca. 20% (w/w) of SN-38 (Fig. 1*A*). The mean particle size of NK012 is 20 nm in diameter with a relatively narrow range (Fig. 1*B*). The releasing rates of SN-38 from NK012 in PBS at 37°C were 57% and 74% at 24 and 48 hours, respectively, and those in 5% glucose solution at 37°C were 1% and 3% at 24 and 48 hours, respectively (Fig. 1*C*). SN-38 is loaded by chemical bonding to the block copolymer. The bonding is phenyl ester bond, which is stable under acidic condition and labile under mild alkaline condition. These results indicate that NK012 can release SN-38 under neutral condition even without the presence of a hydrolytic enzyme and is stable in 5% glucose solution. It is suggested that NK012 is stable before administration and starts to release SN-38, the active component, under physiologic conditions after administration.

Cellular sensitivity of non–small-cell lung cancer and colon cancer cells to SN-38, NK012, and CPT-11. The IC_{50} values of NK012 for the cell lines ranged from 0.009 μmol/L (SBC-3 cells) to 0.16 μmol/L (WiDR cells). The growth inhibitory effects of NK012 are 43- to 340-fold more potent than those of CPT-11, whereas the IC_{50} values of NK012 were 2.3- to 5.8-fold higher than those of SN-38. NK012 exhibited a higher cytotoxic effect against each cell line as compared with CPT-11 (43- to 340-fold sensitivity). On the other hand, the IC_{50} values of NK012 were a little higher than those of SN-38, similar to the cytotoxic feature also reported in a previous study about micellar drugs (ref. 23; Table 1).

Antitumor activity and pharmacokinetic analysis of NK012 and CPT-11 using HT-29–bearing nude mice (experiment 1). Potent activity was observed in mice treated with NK012 at doses of 15 and 30 mg/kg (Fig. 2*A*), although neither CPT-11 at a dose of 66.7 mg/kg/d nor NK012 at a dose of 7.5 mg/kg/d exerted any significant antitumor activity *in vivo*. Comparison of the relative tumor volume at day 21 revealed significant differences between 15 mg/kg/d NK012 and 66.7 mg/kg/d CPT-11 and between 30 mg/kg/d NK012 and 66.7 mg/kg/d CPT-11 ($P < 0.05$). Although treatment-related body weight loss was observed in mice treated with each drug, body weight recovered by day 21 (Fig. 2*B*). These results clearly show the significant *in vivo* activity of NK012 against HT-29.

After injection of CPT-11, the concentrations of CPT-11 and SN-38 for plasma declined rapidly with time in a log-linear fashion. On the other hand, NK012 (polymer-bound SN-38) exhibited slower clearance (Fig. 3*A*). The clearance of NK012 in the HT-29 tumor was significantly slower and the concentration of free SN-38 was maintained at >30 ng/g even at 168 hours after injection (Fig. 3*B*). The pharmacokinetic variables of each drug in the plasma and tumor are depicted in Table 2.

Tumor-to-plasma concentration ratios (Kp) of polymer-bound and free SN-38 increased during the observation period. The highest value of Kp was achieved at 168 hours after administration, 108 for polymer-bound and 11.0 for free SN-38 (Table 3). These results indicate that NK012 can remain in the tumor tissue for a longer period and release free SN-38.

Antitumor activity and the distribution of NK012 and CPT-11 in SBC-3/Neo or SBC-3/VEGF tumors (experiment 2). To determine whether the potent antitumor effect of NK012 is enhanced in the tumors with high vascularity, we used VEGF-secreting cells SBC-3/VEGF. There was no significant difference in the *in vitro* cytotoxic activity of each drug between SBC-3/Neo and SBC-3/VEGF (Fig. 4*A*). SBC-3/VEGF tumors are reddish by gross evaluation as compared with SBC-3/Neo tumors (Fig. 4*B*). Histologic and immunohistochemical (von Willebrand factor) examination revealed that prominent leakage of erythrocytes and high vascularity were observed in SBC-3/VEGF tumor xenografts. On the other hand, SBC-3/Neo tumors have less tumor vasculatures and more interstitial space as compared with SBC-3/VEGF tumors

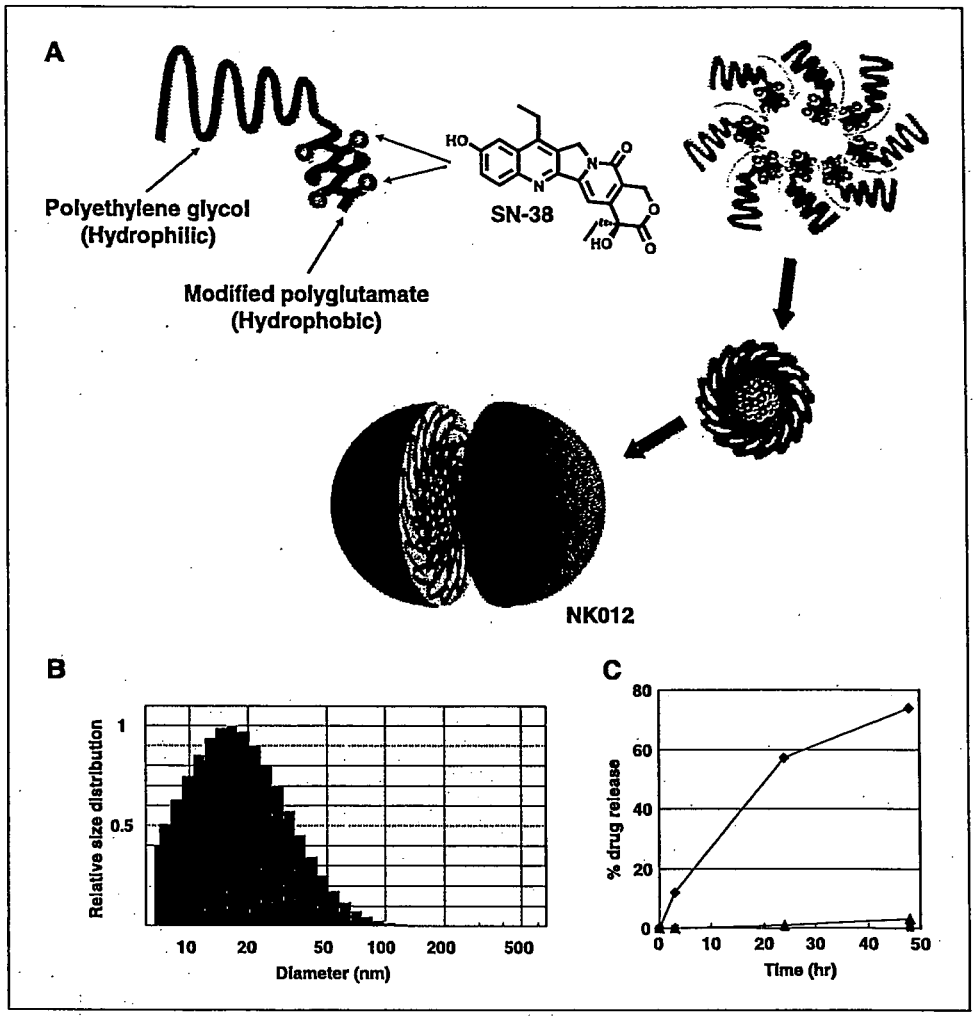

Figure 1. Preparation and characterization of NK012. *A*, schematic structure of NK012. A polymeric micelle carrier of NK012 consists of a block copolymer of PEG (molecular weight of ~12,000) and partially modified polyglutamate (~20 units). PEG (hydrophilic) is believed to be the outer shell and SN-38 was incorporated into the inner core of the micelle. *B*, size distribution of NK012 measured with the dynamic light scattering method. The *Y* axis shows relative particle size distribution. *C*, release of free SN-38 from the micelles in PBS [pH 7.3, 37°C (♦)] or 5% glucose solution [pH 4.6, 20°C (■), 37°C (▲)].

(Fig. 4*B*). Deviating from the ordinary experimental tumor model, tumors were allowed to grow until they became massive in size, ~1.5 cm (Fig. 4*C*), and then the treatment was initiated. NK012 at doses of 15 and 30 mg/kg showed potent antitumor activity against bulky SBC-3/Neo tumors (1,533.1 ± 1,204.7 mm^3) as compared with CPT-11 (Fig. 4*C*). Striking antitumor activity was observed in mice treated with NK012 (Fig. 4*C*) when we compared the antitumor activity of NK012 with that of CPT-11 using SBC-3/VEGF cells. SBC-3/VEGF bulky masses (1,620.7 ± 834.0 mm^3) disappeared in all mice, although relapse 3 months after treatment was noted in one mouse treated with NK012 20 mg/kg. On the other hand, SBC-3/VEGF were not eradicated and rapidly regrew after a partial response in mice treated with CPT-11. Approximately 10% body weight loss was observed in mice treated with 20 mg/kg NK012, but no significant difference was observed in comparison with mice treated with 30 mg/kg CPT-11.

We then examined the distribution of free SN-38 in the SBC-3/Neo and SBC-3/VEGF masses after administration of NK012 and CPT-11. In the case of CPT-11 administration, the concentrations at 1 and 6 hours after the administration were <100 ng/g both in the SBC-3/Neo and SBC-3/VEGF tumors and were almost negligible at 24 hours in both tumors (Fig. 5*A*). There was no significant difference in the concentration between the SBC-3/Neo and SBC-3/VEGF tumors. On the other hand, in the case of NK012 administration, free SN-38 was detectable in the tumors even at 72 hours after the administration. The concentrations of free SN-38 were higher in the SBC-3/VEGF tumors than those in the SBC-3/Neo tumors at any time point during the period of observation (significant at 1, 6, and 24 hours; $P < 0.05$; Fig. 5*A*).

Tissue distribution of SN-38 after administration of NK012 and CPT-11. We examined the concentration-time profile of free SN-38 in various tissues after i.v. administration of NK012 and

Table 1. *In vitro* growth inhibitory activity of SN-38, NK012, and CPT-11 in human lung and colorectal cancer cells (MTT assay)

Cell line	IC_{50} (μmol/L)		
	SN-38	NK012	CPT-11
WiDR	0.046 ± 0.008	0.16 ± 0.014	20.4 ± 1.6
SW480	0.025 ± 0.003	0.11 ± 0.028	31.9 ± 1.3
Lovo	0.0067 ± 0.0012	0.026 ± 0.003	7.24 ± 1.04
HT-29	0.016 ± 0.003	0.068 ± 0.007	23.1 ± 2.63
PC-14	0.044 ± 0.025	0.14 ± 0.021	5.96 ± 0.90
SBC-3	0.0016 ± 0.001	0.0093 ± 0.005	0.72 ± 0.22
A431	0.0081 ± 0.002	0.019 ± 0.007	5.6 ± 1.5

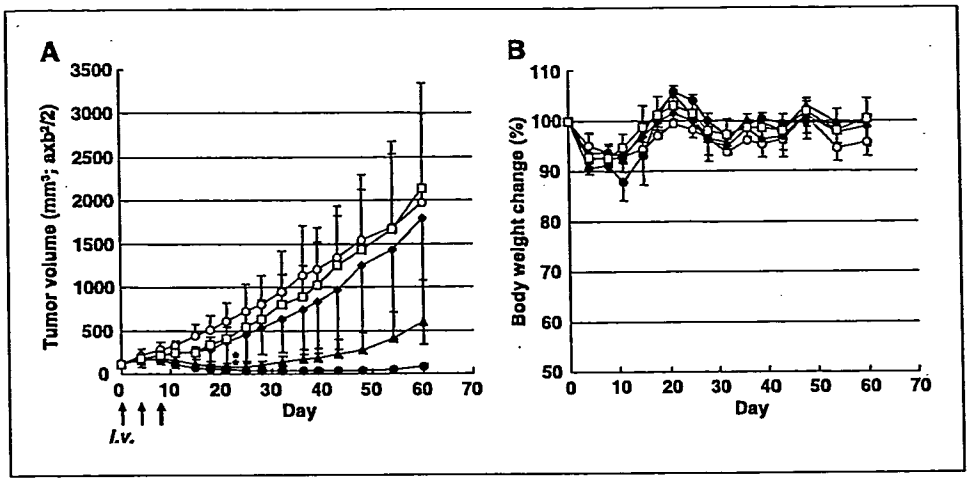

Figure 2. The effect of NK012 and CPT-11 against an HT-29 tumor xenograft. *A*, HT-29 tumor was inoculated s.c. into the flank of mice as described in Materials and Methods. CPT-11 at a dose of 66.7 mg/kg/d (□), NK012 at a dose of 7.5 mg/kg/d (♦), NK012 at a dose of 15 mg/kg/d (▲), or NK012 at a dose of 30 mg/kg/d (●) was administered i.v. on days 0, 4, and 8 (○, no treatment). Tumor volume in mice treated with CPT-11 or NK012. *Points*, mean; *bars*, SD. *, $P < 0.05$. *B*, treatment-related body weight loss occurred in mice treated with CPT-11 and NK012. *Points*, mean; *bars*, SD.

CPT-11. All organs measured exhibited the highest concentration of SN-38 at 1 hour after administration in mice given CPT-11 (Fig. 5*B*). On the other hand, mice given NK012 exhibited prolonged distribution in the liver and spleen (Fig. 5*B*). In a similar manner to other micellar drugs (19, 23), NK012 showed relatively higher accumulation in organs of the reticuloendothelial system. In the lung, kidney, and small intestine, the highest concentration of free SN-38 was achieved at 1 hour after injection of NK012 and the concentration was almost negligible at 24 hours. Although relatively high at 1 hour after administration of NK012 and CPT-11, the concentrations of free SN-38 in the small intestine rapidly decreased. Interestingly, there was no significant difference in the kinetic character of free SN-38 in the small intestine between mice treated with NK012 and CPT-11.

Discussion

The drug-incorporating polymeric micelle has characteristic pharmacokinetic features. These structures are too large to pass through normal vessel walls and evade renal excretion. The outer shell of the drug with PEG diminishes nonspecific capture by the reticuloendothelial system. Therefore, the drug can be expected to achieve a long half-life, which permits a large amount of the drug-incorporating micelles to reach the tumor site through the enhanced permeability and retention effect. The pharmacokinetic study revealed that the plasma AUC of polymer-bound SN-38 after administration of NK012 at a dose of 30 mg/kg to the HT-29-bearing mice was ~200-fold higher than that of CPT-11 at a dose of 66.7 mg/kg. A 14-fold higher AUC of the free SN-38 was achieved in mice given NK012 compared with mice given CPT-11. Prolonged circulation of NK012 in the blood might increase the accumulation of NK012 in a tumor tissue due to the enhanced permeability and retention effect. In fact, the tumor concentration of free SN-38 at 24 hours after administration of NK012 reached 90.4 ng/g and high concentrations were maintained up to 168 hours (53.1 ng/g for 48 hours, 42.6 ng/g for 72 hours, and 35.8 ng/g for 168 hours). This range of concentrations can exert sufficient antitumor activity against tumor cells. On the other hand, the concentration of CPT-11 was only 4.5 ng/g at 24 hours. These results indicate that the enhancement of tumor distribution closely contributes to the potent antitumor activity of NK012 *in vivo*.

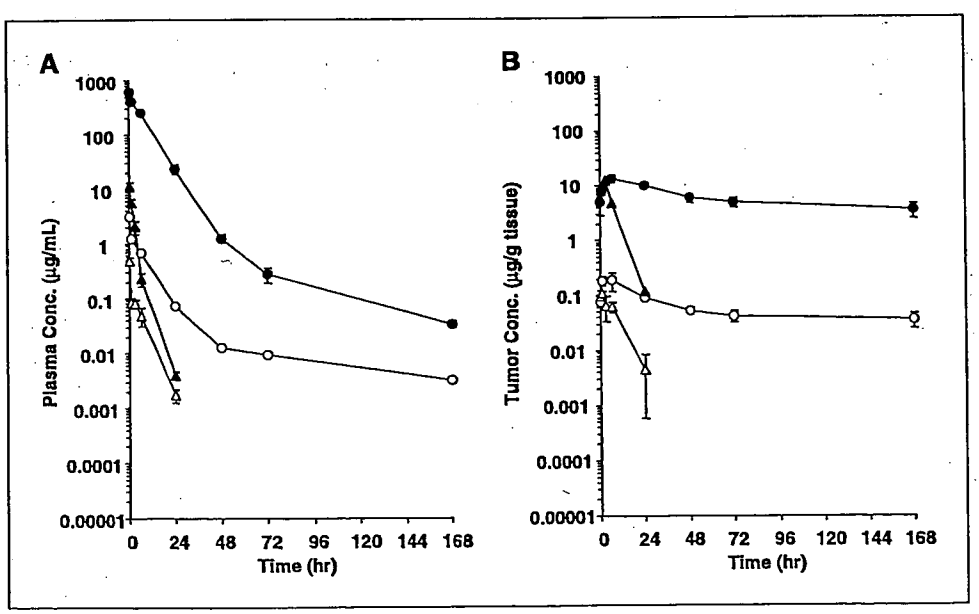

Figure 3. Plasma and tumor concentrations of respective analytes after an i.v. administration of CPT-11 (66.7 mg/kg) or NK012 (30 mg/kg) to HT-29-bearing nude mice. *A*, plasma. *B*, tumor. ●, polymer-bound SN-38; ○, free SN-38 (polymer-unbound SN-38); △, SN-38 converted from CPT-11; ▲, CPT-11.

Table 2. Pharmacokinetic variables of analytes in plasma and tumor after an i.v. administration of NK012 or CPT-11 to nude mice bearing human colon cancer HT-29 cells (NK012, 30 mg/kg; CPT-11, 66.7 mg/kg)

	Test article		C_{max} (μg/mL)	T_{max} (h)	$T_{1/2z}$ (h)	AUC_{last} (μg h/mL)	AUC_{inf} (μg h/mL)	CL_{tot} (mL/h/kg)	V_{ss} (mL/kg)	MRT_{last} (h)	$MRT_{inf.}$ (h)
Plasma	NK012	P-b SN-38*	—†	—	31.4	5,000	5,010	5.99	40.4	6.68	6.74
		P-u SN-38‡	3.10	0.0833	61.7	15.5	15.8	—	—	10.8	15.3
	CPT-11	CPT-11	—	—	3.08	22.1	22.2	3,010	5,420	1.78	1.80
		SN-38	0.488	0.0833	3.76	1.10	1.11	—	—	3.82	4.04
Tumor	NK012	P-b SN-38	13.8	6	—	1,010	—	—	—	62.8	—
		P-u SN-38	0.188	6	—	10.2	—	—	—	58.1	—
	CPT-11	CPT-11	12.6	3	3.36	99.7	100	—	—	4.41	4.55
		SN-38	0.108	1	4.75	1.07	1.10	—	—	5.20	5.92

NOTE: Three female nude mice were used for the analysis of biodistribution of SN-38 and CPT-11 in plasma and tissues. Data were expressed as means.
*Polymer-bound SN-38; SN-38 remaining bound to PEG-PGlu.
†Not determined.
‡Polymer-unbound SN-38; free SN-38 from PEG-PGlu.

Several preclinical studies on cytotoxic agent–incorporating polymeric micelles show their advantage as anticancer agents *in vivo* as compared with drugs of small molecular size (19, 22, 23). Because the advantage of passive targeting has been explained by the enhanced permeability and retention theory, it is essential to elucidate the correlation between the effectiveness of micellar drugs and tumor hypervascularity and hyperpermeability. We hypothesized that a polymeric micelle–based drug carrier could increase its accumulation in the tumor site and could thus enhance the therapeutic efficacy in tumors with high vascularity. To ascertain the hypothesis, we used SBC-3/VEGF. We adopted a bulky tumor model for our *in vivo* experiment to clarify the difference in activity against SBC-3/Neo and SBC-3/VEGF tumors. Histologic examination of SBC-3/VEGF showed hypervascularity and prominent leakage of erythrocytes. On the other hand, SBC-3/Neo showed hypovascularity. Our *in vivo* experiment showed that NK012 obviously enhanced its antitumor activity in SBC-3/VEGF-inplanted mice and eradicated bulky masses. It was thought that the sensitivity of cells to NK012 might not change *in vivo* because the *in vitro* sensitivity of NK012 was almost equivalent between SBC-3/Neo and SBC-3/VEGF cells. When we compared the distribution of NK012 (free SN-38) in the tumor sites, significantly enhanced accumulation was observed in the SBC-3/VEGF tumors. This strongly suggested that the drug distribution throughout the tumor site was enhanced by the hypervascularity and hyperpermeability induced by VEGF, and, subsequently, higher antitumor activity was achieved. High vascular density and enhanced vascular permeability might also be favorable for drug delivery of low molecular weight drugs. However, the SN-38 concentration was not significantly high in SBC-3/VEGF tumors after the administration of CPT-11, and tumors exhibited rapid regrowth after the treatment. We assume that such conventional low molecular size anticancer agents almost disappear from the bloodstream without being subjected to the enhanced permeability and retention effect before they can reach the target organs (solid tumor). The fact of correlation between the blood vessel density in

Table 3. Tumor-to-plasma concentration ratio (Kp) of analytes after an i.v. administration of NK012 (30 mg/kg) to nude mice bearing human colon cancer HT-29 cells

Test article	Analyte		Time after administration (h)						
			0.0833	1	6	24	48	72	168
NK012	P-b SN-38*	Plasma (μg/mL)	612	410	254	23.3	1.25	0.278	0.0333
		Tumor (μg/g)	4.99	8.00	13.8	9.95	5.90	5.03	3.58
		Kp† (mL/g)	0.00815	0.0195	0.0543	0.427	4.72	18.1	108
	P-u SN-38‡	Plasma (μg/mL)	3.10	1.24	0.673	0.0717	0.0127	0.00925	0.00325
		Tumor (μg/g)	0.0763	0.187	0.188	0.0904	0.0531	0.0426	0.0358
		Kp (mL/g)	0.0246	0.151	0.279	1.26	4.18	4.61	11.0

NOTE: Data were expressed as means of three mice.
*Polymer-bound SN-38; SN-38 remaining bound to PEG-PGlu.
†Kp values were calculated on the mean concentrations of three mice.
‡Polymer-unbound SN-38; free SN-38 from PEG-PGlu.

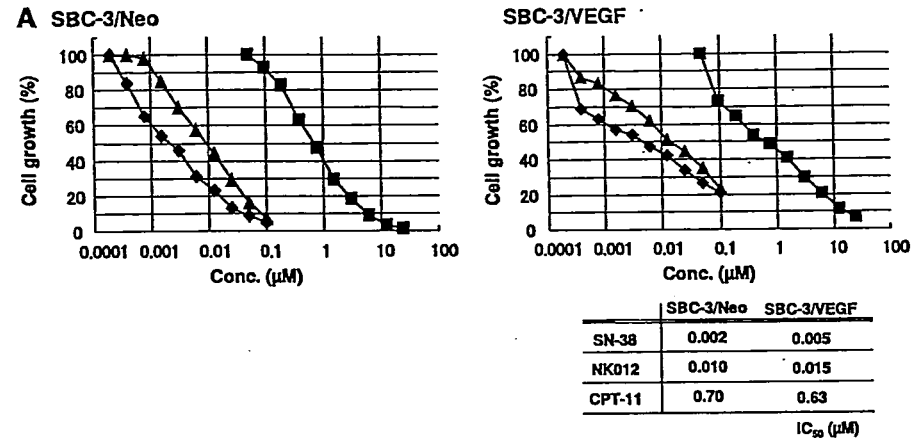

	SBC-3/Neo	SBC-3/VEGF
SN-38	0.002	0.005
NK012	0.010	0.015
CPT-11	0.70	0.63

IC_{50} (μM)

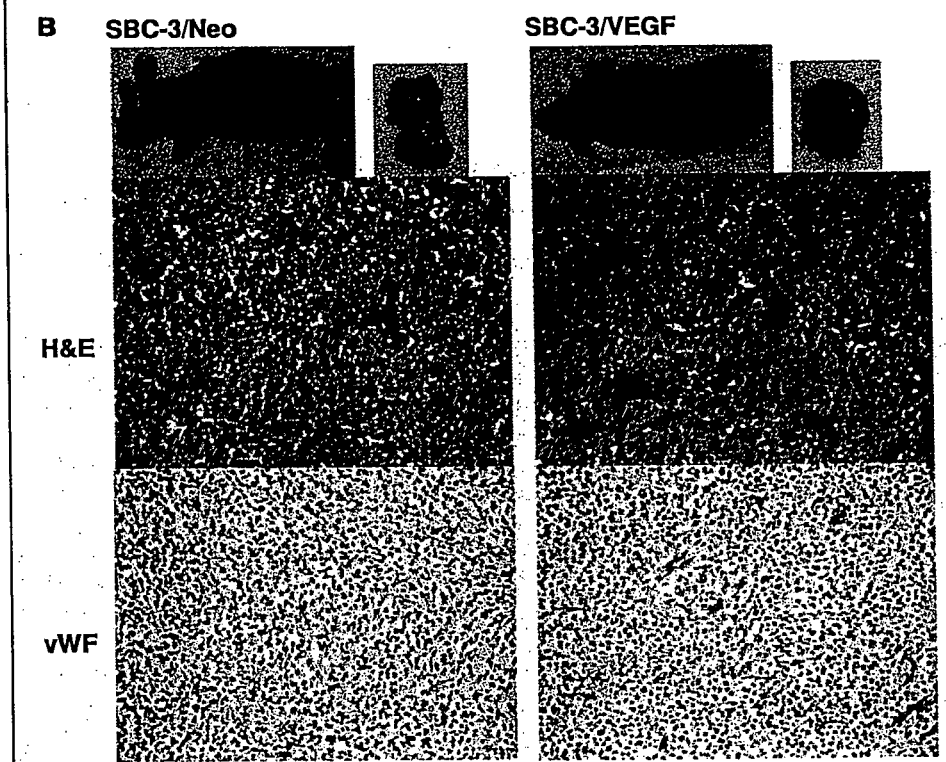

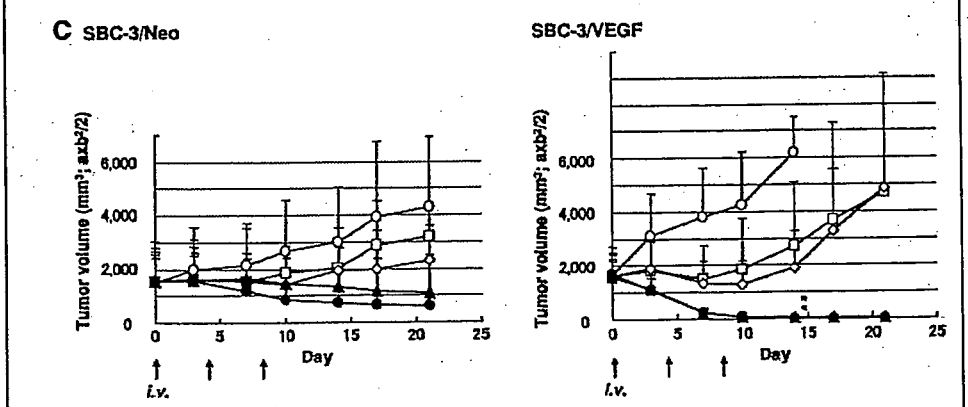

Figure 4. Growth inhibitory effect of NK012, SN-38, and CPT-11 on SBC-3/Neo and SBC-3/VEGF cells. *A*, in *in vitro* experiment, the cells were exposed to the indicated concentrations of each drug for 72 hours. The growth inhibition curves and IC_{50} values for NK012 (▲), SN-38 (♦), and CPT-11 (■) are shown. *B*, representative photographs of massive tumors developed from SBC-3/Neo and SBC-3/VEGF at the time just before treatment initiation. Histologic (H&E, ×20) and immunohistochemical (von Willebrand factor, ×20) examinations for each tumor are shown. *C*, i.v. administration of NK012 or CPT-11 was started when the mean tumor volumes of groups reached a massive size of 1,500 mm^3. The mice were divided into test groups (○, control; □, CPT-11 15 mg/kg/d; ◇, CPT-11 30 mg/kg/d; ▲, NK012 10 mg/kg/d; ●, NK012 20 mg/kg/d). NK012 or CPT-11 was administered i.v. on days 0, 4, and 8. Each group consisted of four mice. *, $P < 0.05$.

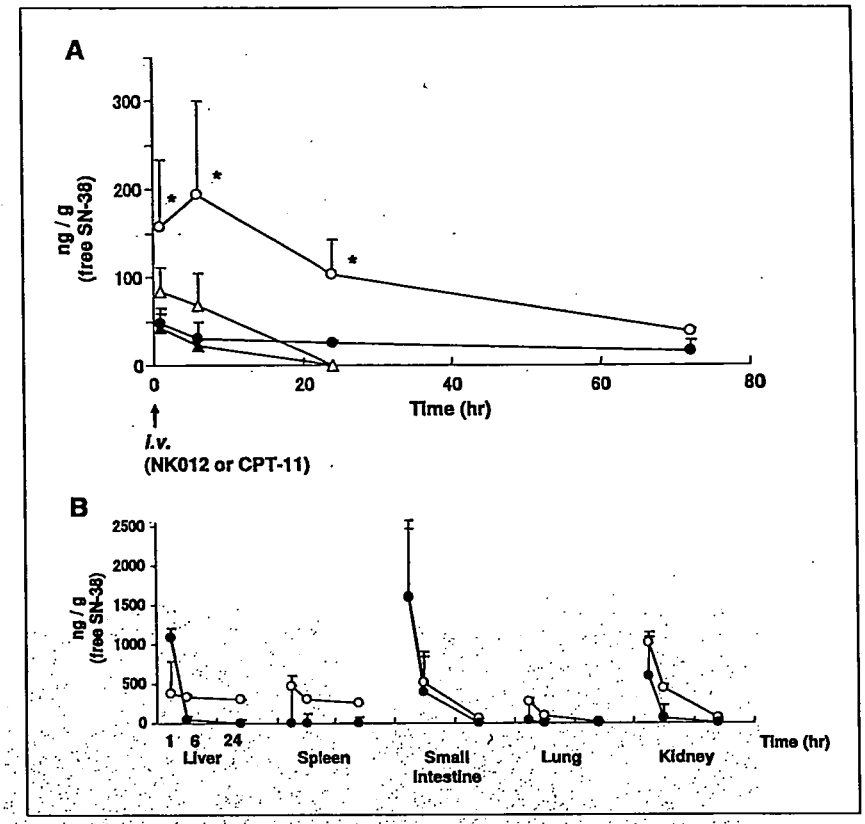

Figure 5. Tissue and tumor distribution of free SN-38 after administration of NK012 and CPT-11. *A*, time profile of free SN-38 concentration in SBC-3/Neo (●, NK012 20 mg/kg/d; ▲, CPT-11 30 mg/kg/d) and SBC-3/VEGF (○,NK012 20 mg/kg/d; △, CPT-11 30 mg/kg/d). NK012 on days 0 and 4 (96 hours) or CPT-11 on day 0 was administered. *, $P < 0.05$. *B*, tissue distribution of free SN-38 after single injection of NK012 at 30 mg/kg (○) and CPT-11 at 40 mg/kg (●).

the tumor mass and poor prognosis for survival in people with various types of cancers (25–28) supports the idea that low molecular weight drugs are not so effective in the treatment of solid tumors, which are rich in blood vessels.

Jain (35) reported that the convective passage of large drug molecules into the core of solid tumors could be impeded by abnormally high interstitial pressures in solid tumors. However, he also considered that low molecular weight anticancer agents might be harmful to normal organs because they can leak out of normal blood vessels freely; he finally concluded that one useful strategy for evading the barriers to drug dispersion would be to inject patients with drug carriers, such as liposome, filled with low molecular weight drugs. NK012 has the potential to allow the effective sustained release of SN-38 inside a tumor following the accumulation of NK012 into tumor tissue. As a matter of fact, substantial amount of SN-38 is expected to be released from the polymeric micelle. Consequently, released SN-38 becomes distributed throughout the tumor tissue and internalizes into cancer cells to kill them.

In recent years, the novel liposome-based formulation of SN-38 (LE-SN38) has been developed (36). LE-SN38 shows promising antitumor activity against various cancer cell lines (37, 38) and a clinical trial to assess its efficacy is now under way (39). The release of SN-38 from LE-SN38 is very slow as compared with NK012, ~1.9% of the drug being released from LE-SN38 in PBS buffer over 120 hours (36). The size of LE-N38 ranges from 150 to 200 nm. On the other hand, the particle size of NK012 is ~20 nm. Interestingly, Unezaki et al. (40) reported that fluorescence-labeled PEG liposomes were densely located outside the tumor vessels and stayed around the vessel walls for 2 days after i.v. injection. These data suggest that the PEG liposome is too large to move freely in the tumor interstitium and too stable to be released easily. The difference in size distribution and the character of the drug release between NK012 and LE-SN38 might influence their clinical effectiveness in the treatment of solid tumors.

One of the major toxicities associated with CPT-11 administration is severe diarrhea. Although the mechanism of the diarrhea has not yet been elucidated, one possible explanation is structural and functional injuries to the gastrointestinal tract owing to the mitotic inhibitory activity of SN-38 and CPT-11. It was reported that the number of episodes of diarrhea had a better correlation with the plasma AUC of SN-38 than with CPT-11 (41). In the present study, no difference in SN-38 accumulations in the small intestine was seen when equimolar NK012 (20 mg/kg) and CPT-11 (30 mg/kg) were administered. We also reported, using a rat mammary tumor model, that NK012 showed significant antitumor effect with diminishing incidence of diarrhea as compared with CPT-11 (42). These results suggest that diarrhea, one of the dose-limiting toxicities of CPT-11, is not augmented by the administration of NK012.

In conclusion, the present data suggest that NK012 possesses a treatment advantage over CPT-11, especially in hypervascular tumors such as renal cell carcinomas, medulloblastomas, and hepatocellular carcinomas. We have now started a phase I clinical trial for NK012 in patients with advanced solid tumors.

Acknowledgments

Received 5/3/2006; revised 7/20/2006; accepted 8/21/2006.

The costs of publication of this article were defrayed in part by the payment of page charges. This article must therefore be hereby marked *advertisement* in accordance with 18 U.S.C. Section 1734 solely to indicate this fact.

References

1. Li LH, Fraser TJ, Olin EJ, Bhuyan BK. Action of camptothecin on mammalian cells in culture. Cancer Res 1972;32:2643–50.
2. Gallo RC, Whang-Peng J, Adamson RH. Studies on the antitumor activity, mechanism of action, and cell cycle effects of camptothecin. Natl Cancer Inst 1971; 46:789–95.
3. Gottlieb JA, Guarino AM, Call JB, Oliverio VT, Block JB. Preliminary pharmacologic and clinical evaluation of camptothecin sodium (NSC-100880). Cancer Chemother Rep 1970;54:461–70.
4. Muggia FM, Creaven PJ, Hansen HH, Cohen MH, Selawry OS. Phase I clinical trial of weekly and daily treatment with camptothecin (NSC-100880): correlation with preclinical studies. Cancer Chemother Rep 1972;56: 515–21.
5. Cunningham D, Pyrhonen S, James RD, et al. Randomised trial of irinotecan plus supportive care versus supportive care alone after fluorouracil failure for patients with metastatic colorectal cancer. Lancet 1998; 352:1413–8.
6. Saltz LB, Cox JV, Blanke C, et al. Irinotecan plus fluorouracil and leucovorin for metastatic colorectal cancer. Irinotecan Study Group. N Engl J Med 2000;343: 905–14.
7. Noda K, Nishiwaki Y, Kawahara M, et al. Irinotecan plus cisplatin compared with etoposide plus cisplatin for extensive small-cell lung cancer. N Engl J Med 2002; 346:85–91.
8. Negoro S, Masuda N, Takada Y, et al. CPT-11 Lung Cancer Study Group West. Randomised phase III trial of irinotecan combined with cisplatin for advanced non-small-cell lung cancer. Br J Cancer 2003; 88:335–41.
9. Bodurka DC, Levenback C, Wolf JK, et al. Phase II trial of irinotecan in patients with metastatic epithelial ovarian cancer or peritoneal cancer. J Clin Oncol 2003; 21:291–7.
10. Takimoto CH, Arbuck SG. Topoisomerase I targeting agents: the camptothecins. In: Chabner BA, Lango DL, editors. Cancer chemotherapy and biotherapy: principal and practice. 3rd ed. Philadelphia (PA): Lippincott Williams & Wilkins; 2001. p. 579–646.
11. Slatter JG, Schaaf LJ, Sams JP, et al. Pharmacokinetics, metabolism, and excretion of irinotecan (CPT-11) following I.V. infusion of [(14)C]CPT-11 in cancer patients. Drug Metab Dispos 2000;28:423–33.
12. Rothenberg ML, Kuhn JG, Burris HA III, et al. Phase I and pharmacokinetic trial of weekly CPT-11. J Clin Oncol 1993;11:2194–204.
13. Guichard S, Terret C, Hennebelle I, et al. CPT-11 converting carboxylesterase and topoisomerase activities in tumour and normal colon and liver tissues. Br J Cancer 1999;80:364–70.
14. Matsumura Y, Maeda H. A new concept for macromolecular therapeutics in cancer chemotherapy: mechanism of tumoritropic accumulation of proteins and the antitumor agent smancs. Cancer Res 1986;46: 6387–92.
15. Dvorak HF, Nagy JA, Dvorak JT, Dvorak AM. Identification and characterization of the blood vessels of solid tumors that are leaky to circulating macromolecules. Am J Pathol 1988;133:95–109.
16. Maeda H, Matsumura Y. Tumoritropic and lymphotropic principles of macromolecular drugs. Crit Rev Ther Drug Carrier Syst 1989;6:193–210.
17. Matsumura Y, Maruo K, Kimura M, Yamamoto T, Konno T, Maeda H. Kinin-generating cascade in advanced cancer patients and *in vitro* study. Jpn J Cancer Res 1991;82:732–41.
18. Yokoyama M, Miyauchi M, Yamada N, et al. Characterization and anticancer activity of the micelle-forming polymeric anticancer drug Adriamycin-conjugated poly(ethylene glycol)-poly(aspartic acid) block copolymer. Cancer Res 1990;50:1693–700.
19. Yokoyama M, Okano T, Sakurai Y, Ekimoto H, Shibazaki C, Kataoka K. Toxicity and antitumor activity against solid tumors of micelle-forming polymeric anticancer drug and its extremely long circulation in blood. Cancer Res 1991;51:3229–36.
20. Kataoka K, Harada A, Nagasaki Y. Block copolymer micelles for drug delivery: design, characterization and biological significance. Adv Drug Deliv Rev 2001;47: 113–31.
21. Matsumura Y, Hamaguchi T, Ura T, et al. Phase I clinical trial and pharmacokinetic evaluation of NK911, a micelle-encapsulated doxorubicin. Br J Cancer 2004;91: 1775–81.
22. Hamaguchi T, Matsumura Y, Suzuki M, et al. NK105, a paclitaxel-incorporating micellar nanoparticle formulation, can extend *in vivo* antitumour activity and reduce the neurotoxicity of paclitaxel. Br J Cancer 2005; 92:1240–6.
23. Uchino H, Matsumura Y, Negishi T, et al. Cisplatin-incorporating polymeric micelles (NC-6004) can reduce nephrotoxicity and neurotoxicity of cisplatin in rats. Br J Cancer 2005;93:678–87.
24. Folkman J. Anti-angiogenesis: new concept for therapy of solid tumors. Ann Surg 1972;175:409–16.
25. Gasparini G, Harris AL. Clinical importance of the determination of tumor angiogenesis in breast carcinoma: much more than a new prognostic tool. J Clin Oncol 1995;13:765–82.
26. Dickinson AJ, Fox SB, Persad RA, Hollyer J, Sibley GN, Harris AL. Quantification of angiogenesis as an independent predictor of prognosis in invasive bladder carcinomas. Br J Urol 1994;74:762–6.
27. Takahashi Y, Kitadai Y, Bucana CD, Cleary KR, Ellis LM. Expression of vascular endothelial growth factor and its receptor, KDR, correlates with vascularity, metastasis, and proliferation of human colon cancer. Cancer Res 1995;55:3964–8.
28. Williams JK, Carlson GW, Cohen C, Derose PB, Hunter S, Jurkiewicz MJ. Tumor angiogenesis as a prognostic factor in oral cavity tumors. Am J Surg 1994; 168:373–80.
29. Natsume T, Watanabe J, Koh Y, et al. Antitumor activity of TZT-1027 (Soblidotin) against vascular endothelial growth factor-secreting human lung cancer *in vivo*. Cancer Sci 2003;94:826–33.
30. Stacker SA, Caesar C, Baldwin ME, et al. VEGF-D promotes the metastatic spread of tumor cells via the lymphatics. Nat Med 2001;7:186–91.
31. Amoroso A, Del Porto F, Di Monaco C, Manfredini P, Afeltra A. Vascular endothelial growth factor: a key mediator of neoangiogenesis. A review. Eur Rev Med Pharmacol Sci 1997;1:17–25.
32. Cabral H, Nishiyama N, Okazaki S, Koyama H, Kataoka K. Preparation and biological properties of dichloro(1,2-diaminocyclohexane)platinum(II) (DACHPt)-loaded polymeric micelles. J Controlled Res 2005;101: 223–32.
33. Nishiyama N, Yokoyama M, Aoyagi T, Okano T, Sakurai Y, Kataoka K. Preparation and characterization of self-assembled polymer-metal complex micelle from *cis*-dichlorodiammineplatinum(II) and poly(ethylene glycol)-poly(α,β-aspartic acid) block copolymer in an aqueous medium. Langmuir 1999;15:377–83.
34. Kawato Y, Furuta T, Aonuma M, Yasuoka M, Yokokura T, Matsumoto K. Antitumor activity of a camptothecin derivative, CPT-11, against human tumor xenografts in nude mice. Cancer Chemother Pharmacol 1991;28:192–8.
35. Jain RK. Barriers to drug delivery in solid tumors. Sci Am 1994;271:58–65.
36. Zhang JA, Xuan T, Parmar M, et al. Development and characterization of a novel liposome-based formulation of SN-38. Int J Pharm 2004;270:93–107.
37. Lei S, Chien PY, Sheikh S, Zhang A, Ali S, Ahmad I. Enhanced therapeutic efficacy of a novel liposome-based formulation of SN-38 against human tumor models in SCID mice. Anticancer Drugs 2004;15:773–8.
38. Pal A, Khan S, Wang YF, et al. Preclinical safety, pharmacokinetics and antitumor efficacy profile of liposome-entrapped SN-38 formulation. Anticancer Res 2005;25:331–41.
39. Kraut EH, Fishman MN, LoRusso PM, et al. Final result of a phase I study of liposome encapsulated SN-38 (LE-SN38): safety, pharmacogenomics, pharmacokinetics, and tumor response [abstract 2017]. Proc Am Soc Clin Oncol 2005;23:139s.
40. Unezaki S, Maruyama K, Hosoda JI, et al. Direct measurement of the extravasation of polyethyleneglycol-coated liposomes into solid tumor tissue by *in vivo* fluorescence microscopy. Int J Pharmaceut 1996;144: 11–7.
41. Sasaki Y, Yoshida Y, Sudoh K, et al. Pharmacological correlation between total drug concentration and lactones of CPT-11 and SN-38 in patients treated with CPT-11. Jpn J Cancer Res 1995;86:111–6.
42. Onda T, Nakamura I, Seno C, et al. Superior antitumor activity of NK012, 7-ethyl-10-hydroxycamptothecin-incorporating micellar nanoparticle, to irrinotecan [abstract 3062]. Proc Am Assoc Cancer Res 2006;47: 720s.

Available online at www.sciencedirect.com
ScienceDirect
Journal of Controlled Release 117 (2007) 130–136
journal of controlled release
www.elsevier.com/locate/jconrel

Gene delivery by combination of novel liposomal bubbles with perfluoropropane and ultrasound

Ryo Suzuki [a,1], Tomoko Takizawa [a,1], Yoichi Negishi [b,1], Kosuke Hagisawa [c,1], Kumiko Tanaka [a], Kaori Sawamura [a], Naoki Utoguchi [a], Toshihiko Nishioka [d], Kazuo Maruyama [a,*]

[a] *Department of Biopharmaceutics, School of Pharmaceutical Sciences, Teikyo University, 1091-1 Suwarashi, Sagamiko-cho, Sagamihara, Kanagawa, Japan*
[b] *School of Pharmacy, Tokyo University of Pharmacy and Life Science, Hachioji, Tokyo, Japan*
[c] *Department of Medical Engineering, National Defense Medical College, Tokorozawa, Saitama, Japan*
[d] *Division of Cardiology, Saitama Medical Center, Saitama Medical School, Tsujido, Kamoda, Kawagoe, Saitama, Japan*

Received 12 May 2006; accepted 14 September 2006
Available online 26 September 2006

Abstract

Microbubbles and ultrasound have recently been investigated with a view to improving the transfection efficiency of non-viral gene delivery systems. However, microbubbles are unstable and their targeting ability is insufficient for clinical use. To circumvent these problems, we developed novel polyethyleneglycol (PEG) modified liposomes (Bubble liposomes) containing perfluoropropane, which is an ultrasound imaging gas. Here, we used ultrasound to induce cavitation in Bubble liposomes and then investigated their ability to deliver genes in vitro and in vivo. Bubble liposomes could deliver plasmid DNA to many cell types without cytotoxicity. Additionally, in vivo gene delivery, Bubble liposomes were more effective delivery into femoral artery than lipofection method. Thus, Bubble liposomes might be efficient and novel non-viral tools for gene delivery.

Keywords: Liposomes; Gene delivery; Ultrasound; Cavitation; Non-viral vector

1. Introduction

Gene therapy has a potential in the treatment of cancer and diseases that are due to genomic causes. In addition, at present gene therapy is applied into cardiovascular diseases. Especially, in arteriosclerosis obliterans (ASO), vascular endothelial growth factor and hepatocyte growth factor (HGF) gene therapies have been reported to have beneficial effects. Viral vectors are efficient carriers of genes for transduction, but some problems have become evident [1–3]. Delivery vectors that are highly potent in terms of gene transduction efficiency should also be safe and easy to apply. Non-viral vectors have recently received focus as gene carriers [4], but their transduction efficiency is very low. Efforts have recently been directed towards improving this aspect [5–9].

Microbubbles, which are contrast agents for medical ultrasound imaging, improve transfection efficiency after ultrasound-induced cavitation [10–15]. However, microbubbles are generally unstable and their mean diameter of around 1–6 μm is too large for intravascular applications [16]. Moreover, functional particles such as targeting molecules are difficult to modify on the surface of microbubbles. Therefore, microbubbles should generally be smaller than red blood cells, stable after injection into the blood and ultimately, their surface should be easily modified with functional molecules for targeting.

Liposomes have some advantages as drug, antigen and gene delivery carriers [6,7,17–25]. Their size can be easily controlled and they can be modified to add a targeting function [20–24]. Therefore, we considered that Bubble liposomes could be novel gene delivery agents. Based on liposome technology, we developed novel Bubble liposomes containing the ultrasound

* Corresponding author. Tel.: +81 42 685 3724; fax: +81 42 685 3432.
E-mail address: maruyama@pharm.teikyo-u.ac.jp (K. Maruyama).
[1] The first four authors contributed equally to this work.

0168-3659/$ - see front matter © 2006 Elsevier B.V. All rights reserved.
doi:10.1016/j.jconrel.2006.09.008

imaging gas, perfluoropropane [26,27]. Here, we assessed the feasibility of Bubble liposomes for gene delivery after cavitation induced by ultrasound.

2. Materials and methods

2.1. Cells

The African green monkey kidney fibroblast cell line, COS-7, was cultured in Dulbecco's modified Eagle's medium (DMEM; Sigma Chemical Co., St. Louis, MO) supplemented with 10% heat-inactivated fetal bovine serum (FBS, GIBCO, Invitrogen Co., Carlsbad, CA). Meth-A fibrosarcoma cells and Jurkat cells, a human T cell line, were cultured with RPMI-1640 (Sigma Chemical Co., St. Louis, MO) supplemented with 10% heat-inactivated FBS. Colon 26 cells derived from a mouse colon adenocarcinoma, were cultured with RPMI-1640 (Sigma Chemical Co., St. Louis, MO) supplemented with 10% heat-inactivated FBS and 2.5% HEPES. B16BL6 cells were cultured with Eagle's medium (MEM) supplemented with 10% heat-inactivated FBS. Human umbilical vein endothelial cells (HUVEC, Kurabo Industries, Osaka, Japan) were cultured in a DMEM and medium 199 mixture with 15% heat-inactivated FBS, heparin (3.25 U/mL) and endothelial cell growth supplement (ECGS, Sigma Chemical Co., St. Louis, MO). All culture media contained 100 U/ml penicillin (Wako Pure Chemical Industries, Ltd., Osaka, Japan) and 100 μg/ml streptomycin (Wako Pure Chemical Industries, Ltd., Osaka, Japan).

2.2. Preparation of liposomes and Bubble liposomes

Liposomes composed of 1,2-distearoyl-sn-glycero-phosphatidylcholine (DSPC) (NOF Corporation, Tokyo, Japan) and 1,2-distearoyl-sn-glycero-3-phosphatidyl-ethanolamine-methoxy-polyethyleneglycol (DSPE-PEG (2k)-OMe) (NOF Corporation, Tokyo, Japan) (94:6 (m/m)) were prepared by reverse phase evaporation. In brief, all reagents were dissolved in 9:1 (v/v) chloroform/methanol. Physiological saline was added into the lipid solution. After that, the mixture was sonicated and evaporated at 65 °C. The solvent was completely removed, and the size of the liposomes was adjusted to less than 200 nm using extruding equipment (Northern Lipids Inc., Vancouver, BC) and sizing filter (pore size: 200 nm, 100 nm) (Nuclepore Track-Etch Membrane, Whatman plc, UK). After sizing, liposomes were passed through a 0.45 μm pore size filter (MILLEX HV filter unit, Durapore PVDF membrane, Millipore Corporation, MA) to sterilize. Lipid concentration was measured with Phospholipid C test Wako (Wako Pure Chemical Industries, Ltd., Osaka, Japan). Bubble liposomes were prepared from liposomes and perfluoropropane gas (Takachiho Chemical Ind. Co. Ltd., Tokyo, Japan). In brief, 5 mL sterilized vials containing 2 mL of liposome suspension (lipid concentration: 1 mg/mL) were filled with perfluoropropane gas, capped and then pressured with 7.5 mL of perfluoropropane gas. The vial was placed in a bath-type sonicator (42 kHz, 100 W) (BRANSONIC 2510J-DTH, Branson Ultrasonics Co., Danbury, CT) for 5 min to form Bubble liposomes.

2.3. Ultrasound imaging in vitro

Bubble liposomes and PEG-liposomes (1 mg/mL, 200 μL) were placed into latex tubes filled with degassed PBS (10 mL) in a water bath. The probe (9 MHz) of an ultrasound imaging machine (UF-750XT, Fukuda Denshi Co Ltd., Tokyo, Japan) was positioned under the bath and Bubble liposomes and PEG-liposomes were imaged.

2.4. Cytotoxicity of Bubble liposomes and ultrasound to COS-7 cells

COS-7 cells (1×10^5 cells) and Bubble liposomes (60 μg) mixed with 500 μL of culture medium in 2 mL polypropylene tubes (BMBio, Tokyo, Japan) were exposed to ultrasound (frequency, 2 MHz; duty, 50%; burst rate, 2 Hz) for 10 s using a Sonopore 3000 (NEPA GENE, CO., LTD., Chiba, Japan). The cells were washed with culture medium and resuspended in 1 mL of the same medium. Cell suspensions (100 μL) were seeded in 96-well plates and incubated for 24 h. Cell viability was assayed using MTT [3-(4,5-s-dimethylthiazol-2-yl)-2,5-diphenyl tetrazolium bromide] (Dojindo, Kumamoto, Japan) as described by Mosmann with minor modifications [28]. Briefly, MTT (5 mg/mL, 10 μL) was added to each well and the cells were incubated at 37 °C for 4 h. The formazan product was dissolved in 100 μL of 10% sodium dodecyl sulfate (SDS) (Wako Pure Chemical Ind. Co., Ltd. Osaka, Japan) containing 15 mM HCl. Color intensity was measured using a microplate reader (POWERSCAN HT; Dainippon Pharmaceutical, Osaka, Japan) at test and reference wavelengths of 595 and 655 nm, respectively.

2.5. Damage to plasmid DNA caused by Bubble liposomes and ultrasound

Plasmid DNA (pCMV-Luc; 1 μg) dissolved in 500 μL of Opti-MEM (Invitrogen Corporation, Carlsbad, CA) was exposed to ultrasound with or without Bubble liposomes (60 μg) under the following conditions: frequency, 2 MHz; duty, 50%; intensity, 0, 0.1, 2.5, 4.5 and 6.0 W/cm^2, time, 0, 10, 30 s. As control, we used naked plasmid DNA with and without Bubble liposomes. In this group, plasmid DNA and Bubble liposomes were contacted for 30 s. Bubble liposomes were then removed using phenol/chloroform and plasmid DNA recovered by ethanol precipitation was dissolved in TE buffer and resolved by electrophoresis in 0.7% agarose gels.

2.6. Transfection of plasmid DNA into cells using Bubble liposomes

Plasmid DNA (pCMV-Luc or pEGFP-C1 (Clontech Laboratories, Inc., Mountain View, CA)), cells and Bubble liposomes were suspended in culture medium with 10% FBS in 2 mL polypropylene tubes. Ultrasound was exposed under various conditions through a probe placed in the suspension. The cells were washed twice with PBS and then resuspended in fresh culture medium. And the cells were cultured in 48-wells plate or chamber slide glass (ASAHI TECHNOGLASS CO., Chiba, Japan).

2.7. In vivo gene delivery into the femoral artery of mice

Three hundred μL of Plasmid DNA (pCMV-Luc; 10 μg) with or without Bubble liposomes (250 μg) suspension was injected into femoral artery of ddY mice (6 weeks age, male) using 30-gauge needle (M-S SURGICAL MFG. CO., LTD., Tokyo, Japan). In the same time, ultrasound (frequency, 1 MHz, duty, 50%; intensity, 1.0 W/cm^2, time, 2 min) was transdermally exposed to downstream of injection site. In other samples, plasmid DNA (pCMV-Luc, 10 μg) and Lipofectamine 2000 (50 μg) (Invitrogen Corporation, Carlsbad, CA) were mixed and complexed according to manual of Lipofectamine 2000. The complex was suspended in PBS (300 μL) and injected into femoral artery of mice. After 2 days of injection, the mice were sacrificed and the femoral artery of ultrasound exposure area was collected. Then, the artery was homogenated in the lysis buffer (0.1 M Tris-HCl (pH 7.8), 0.1% Triton X-100, 2 mM EDTA).

2.8. Measurement of luciferase and EGFP expression

Luciferase activity was measured using a luciferase assay system (Promega, Madison, WI) and a luminometer (TD-20/20, Turner Designs, Sunnyvale, CA, USA), is indicated as relative light units (RLU) per mg protein. In the Luciferase in vivo imaging, D-luciferin (150 mg/kg) was intraperitoneally injected into mice. After 10 min of injection, luciferase expression was imaged with luciferase in vivo imaging system (IVIS system 100, Xenogen Corporation, Alameda, CA). EGFP expression

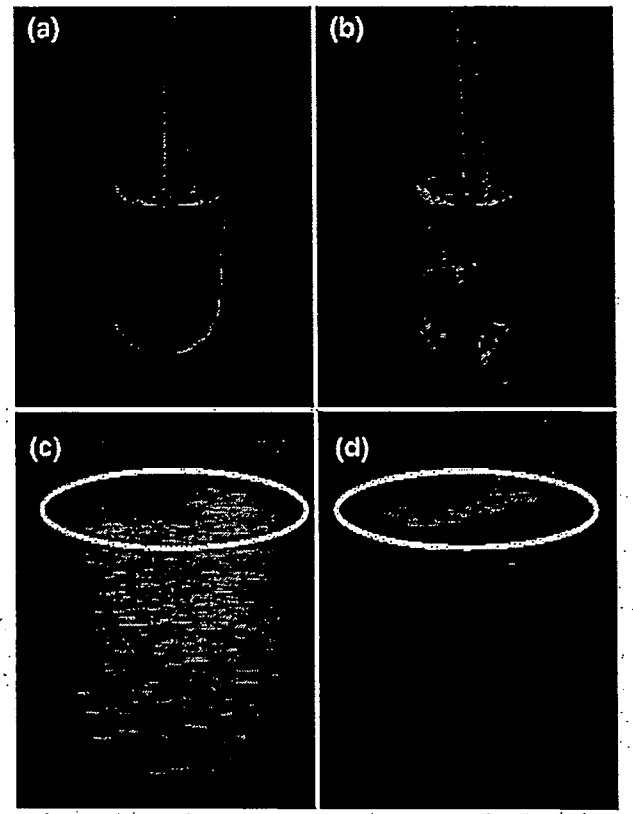

Fig. 2. Cavitation of Bubble liposomes exposed to ultrasound. Naked (a, b) and ultrasonographic (c, d) images of Bubble liposomes. Ultrasonic probe (circle) positioned in Bubble liposome suspension exposed 2.5 W/cm^2 of ultrasound for 10 s. Images were observed before (a, c) and after ultrasound (b, d).

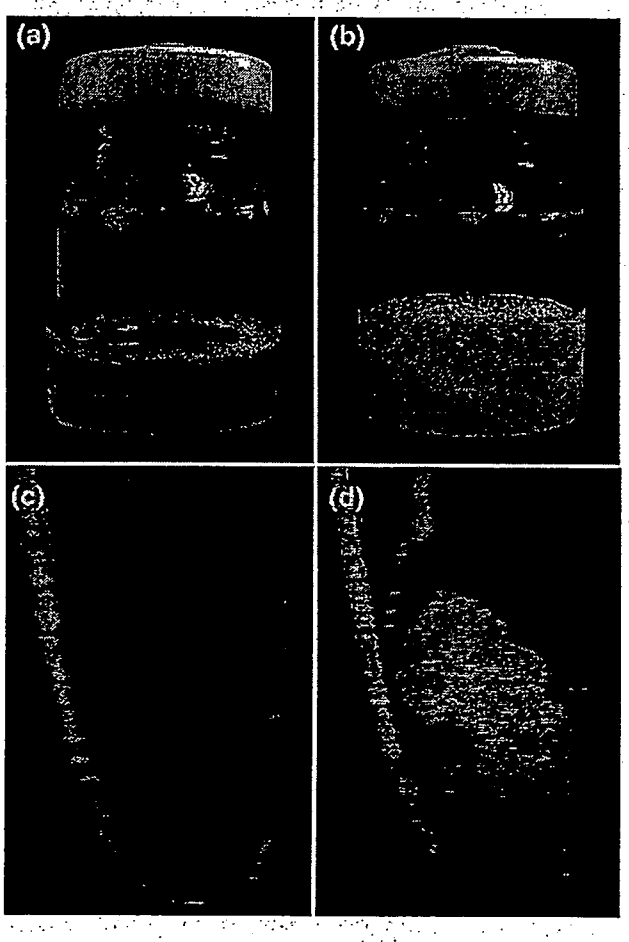

Fig. 1. Aspect and ultrasonography of PEG-liposomes and Bubble liposomes. Aspects of PEG-liposomes (a) and Bubble liposomes (b). PEG-liposomes sonicated with perfluoropropane gas became to Bubble liposomes in the vial. Ultrasonographic images of PEG- (c) and Bubble (d) liposomes.

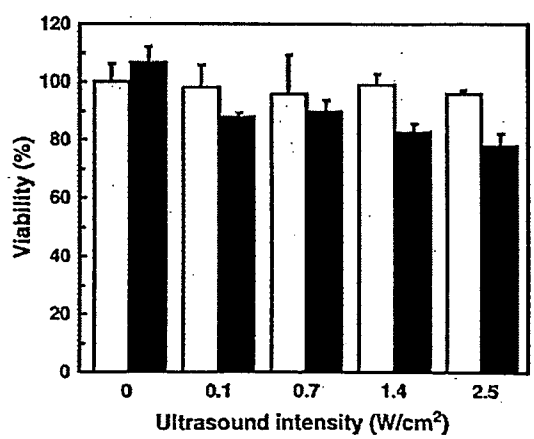

Fig. 3. Viability of COS-7 cells exposed with US and Bubble liposomes. COS-7 cells were exposed to ultrasound under various intensities with (■) or without (□) Bubble liposomes and then cultured for 24 h. Cell viability was assessed by MTT assays. Data are shown as means±S.D. (n=3).

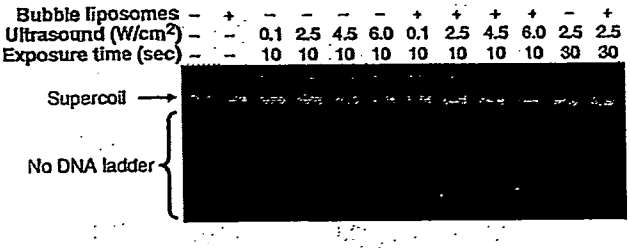

Fig. 4. Plasmid pCMV-Luc exposed to ultrasound under various conditions with or without Bubble liposomes. After exposure to ultrasound, Bubble liposomes were removed using phenol/chloroform and then pCMV-Luc was conventionally precipitated with ethanol. The precipitate was dissolved in TE buffer and resolved by electrophoresis in 0.7% agarose gels.

was observed with fluorescence microscopy (Leica MICROSYSTEMS, Wetzlar, Germany).

3. Results

3.1. Features of Bubble liposomes

Liposomes placed in vials that were supercharged with perfluoropropane gas were sonicated in a bath sonicator. The suspension of Bubble liposomes became cloudier than the original liposome suspension (Fig. 1). On the other hand, when vials were supercharged without perfluoropropane gas or with perfluoropropane gas at atmospheric pressure and then sonicated, the appearance of the liposomes did not change (data not shown). Therefore, sonicating the liposomes under high pressure with perfluoropropane gas was critical. Ultrasound imaging confirmed that the perfluoropropane gas was in fact trapped within the Bubble liposomes. Echo signals were apparently enhanced in Bubble liposomes compared with conventional PEG-liposomes. In addition, ultrasound (2 MHz, 2.5 W/cm^2) disrupted Bubble liposomes by inducing cavitations and then echo signals of these liposomes decreased (Fig. 2).

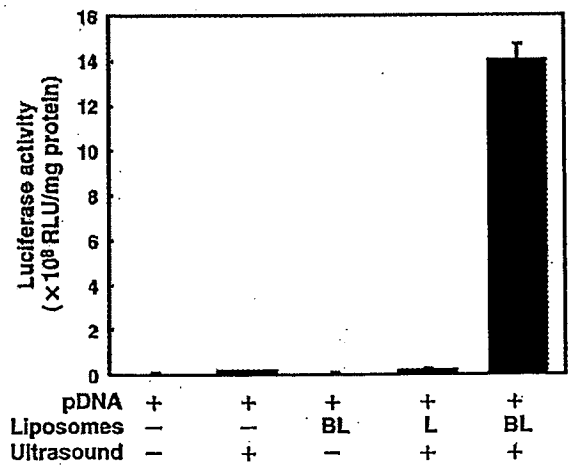

Fig. 5. Luciferase expression in COS-7 cells transfected by ultrasound with Bubble liposomes. COS-7 cells (1×10^5 cells/500 μL) mixed with pCMV-Luc (5 μg) and Bubble liposomes (60 μg) were exposed to ultrasound (frequency, 2 MHz; Duty, 50%; burst rate, 2 Hz; intensity, 2.5 W/cm^2; time 10 s). The cells were washed and cultured for 2 days and then luciferase activity was determined as described in Materials and methods. Data are shown as means±S.D. (n=3). BL, Bubble liposomes; L, PEG-liposomes.

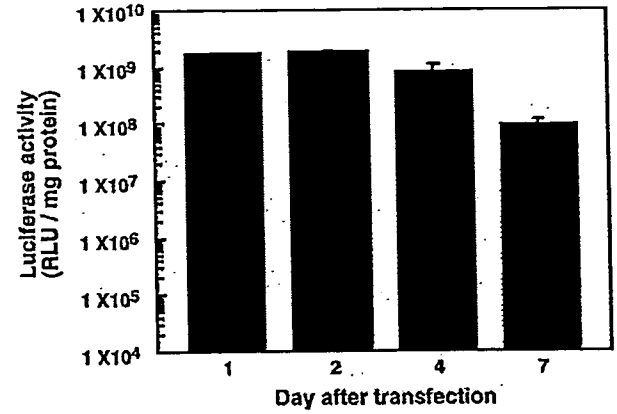

Fig. 6. Duration of luciferase expression in COS-7 cells transfected using ultrasound with Bubble liposomes. COS-7 cells (1×10^5 cells/500 μL) mixed with pCMV-Luc (5 μg) and Bubble liposomes (60 μg) were exposed to ultrasound under the following conditions: frequency, 2 MHz; duty, 50%; burst rate, 2 Hz; intensity, 2.5 W/cm^2; time 10 s). The cells were washed and cultured for 1, 2, 4, 7 days. After that, luciferase activity was determined as described in Materials and methods. Each data represents the mean±S.D. (n=3).

Cavitations of the Bubble liposomes were also visually obvious since suspensions were clarified after exposure to ultrasound (Fig. 2).

3.2. Effects of cavitation induced in Bubble liposomes and ultrasound exposure on COS-7 cells and plasmid DNA

Heat and jet streams are generally induced with cavitation, which might damage cells and plasmid DNA. We therefore examined the effects of ultrasound on cells and plasmid DNA with or without Bubble liposomes. Ultrasound did not damage COS-7 cells in the absence of Bubble liposomes (Fig. 3) and only slightly affected the cells even when the amount of ultrasound was sufficient to induce cavitation of the Bubble liposomes. We also examined the effects of cavitation on plasmid DNA after ultrasound with and without Bubble liposomes using agarose gel electrophoresis (Fig. 4). The results showed that

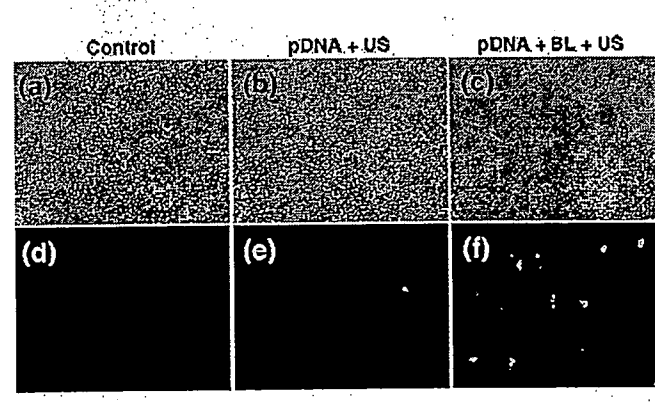

Fig. 7. EGFP expression in COS-7 cells transfected with Bubble liposomes and ultrasound exposure. COS-7 cells (1×10^5 cells/500 μL/tube) were mixed with pEGFP-C1 (5 μg) and Bubble liposomes (60 μg). The cell mixture was exposed to ultrasound (frequency, 2 MHz; duty, 50%; burst rate, 2 Hz; intensity, 2.5 W/cm^2; time 10 s). The cells were washed and cultured for 2 days. Thereafter, EGFP expression was examined by fluorescence microscopy original mgnification X100. Phase contrast, (a-c); Fluorecence (d-f). BL, Bubble liposomes; US, Ultrasound.

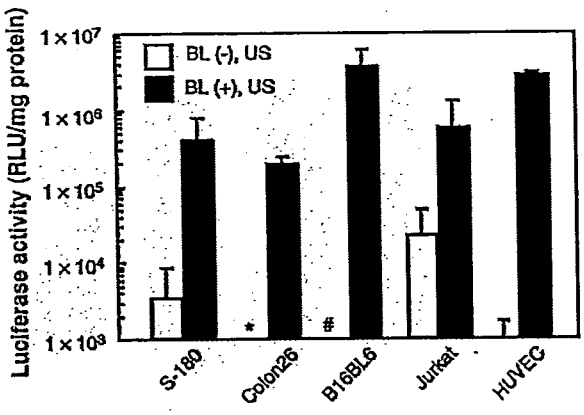

Fig. 8. Luciferase expression in various types of cells transfected using Bubble liposomes and ultrasound. Cells (1×10^5 cells/500 μL) mixed with pCMV-Luc (5 μg) and Bubble liposomes (60 μg) were exposed or not to ultrasound (frequency, 2 MHz; duty, 50%; burst rate, 2 Hz; intensity, 2.5 W/cm^2; time 10 s). The cells were washed and cultured for 2 days. Thereafter, luciferase activity was determined as described in Materials and methods. Data are shown as means±S.D. (n=3). BL, Bubble liposomes; US, Ultrasound. *<10^3 RLU/mg protein, #<10^0 RLU/mg protein.

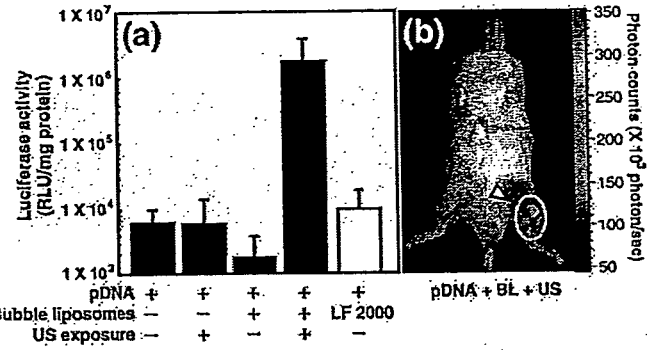

Fig. 10. Gene delivery to femoral artery with Bubble liposomes. Each sample containing plasmid DNA 10 μg was injected into femoral artery. In the same time, ultrasound (frequency, 1 MHz; duty, 50%; burst rate, 2 Hz; intensity, 1 W/cm^2; time 2 min) was exposed to the downstream area of injection site. (a) Luciferase expression in femoral artery of the ultrasound exposure area at 2 days after transfection, Luciferase expression was determined as described in Materials and methods. Data are shown as means±S.D. (n=5). (LF2000: Lipofectamine 2000) (b) In vivo luciferase imaging at 2 days after transfection in the mouse treated with plasmid DNA, Bubble liposomes and ultrasound exposure. The photon counts are indicated by the pseudo-color scales. Arrow head shows injection site and circle shows ultrasound exposure area BL, Bubble liposomes; US, Ultrasound.

10–30 s of ultrasound did not degrade plasmid DNA regardless of the presence or absence of Bubble liposomes.

3.3. Gene transduction with Bubble liposomes and ultrasound

We examined the transduction of naked plasmid DNA into COS-7 cells by Bubble liposomes and/or ultrasound (Fig. 5). Levels of luciferase expression were much higher after ultrasound in the presence, than in the absence of Bubble liposomes. We then examined the profile of gene expression with transfection using Bubble liposomes and ultrasound (Fig. 6). Gene expression peaked 2 days after transfection and then gradually decreased, but remained detectable at 7 days after transfection.

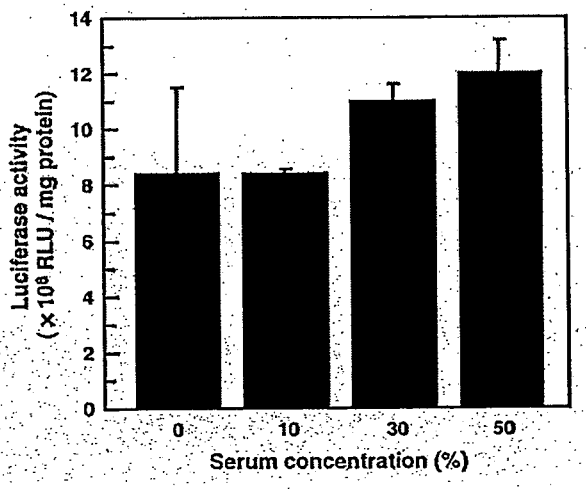

Fig. 9. Effect of serum on transfection efficiency of Bubble liposomes. COS-7 cells (1×10^5 cells/500 μL) mixed with pCMV-Luc (0.25 μg) and Bubble liposomes (60 μg) were exposed to ultrasound (frequency, 2 MHz; duty, 50%; burst rate, 2 Hz; intensity, 2.5 W/cm^2; time 10 s) in the absence or the presence of serum (0, 10, 30, 50%). The cells were washed and cultured for 2 days. Thereafter, luciferase activity was determined as described in Materials and methods. Data are shown as means±S.D. (n=3).

Fig. 7 shows the efficiency of transgene delivery using the EGFP gene expression system. The numbers of EGFP-positive cells significantly increased after ultrasound in the presence, compared with the absence of Bubble liposomes. We also examined the feasibility of gene transduction into S-180, Colon 26, B16BL6, Jurkat cells and human umbilical vein endothelial cells (HUVEC). Fig. 8 shows that Bubble liposomes with ultrasound more effectively transduced luciferase gene into all of these types of cells than ultrasound alone.

Considering in vivo gene delivery with Bubble liposomes, it is necessary to deliver plasmid DNA into cells in presence of serum. Then, we examined about the effect of serum on gene delivery with Bubble liposomes (Fig. 9). Gene expression with Bubble liposomes was not affected even in the presence of serum.

3.4. In vivo gene delivery with Bubble liposomes

To evaluate the ability of Bubble liposomes to in vivo gene delivery, we attempted to deliver plasmid DNA with Bubble liposomes into femoral artery. In this study, we also examined the gene delivery with conventional lipofection method (Fig. 10(a)). The gene expression with ultrasound or Bubble liposomes was low level. In addition, the gene expression was very low even in using Lipofectamine 2000. However, in the combination of Bubble liposomes and ultrasound exposure, gene expression was higher than other groups. And the gene expression was observed at only area of ultrasound exposure (Fig. 10 (b)).

4. Discussion

Plasmid DNA shows promise as a safe and clinically acceptable route for delivering gene therapy, but it must be effective and site-specific. Microbubbles and ultrasound have recently been proposed for gene delivery, since microbubble-

enhanced ultrasound can alter cell membrane permeability for a short time due to sonoporation, which allows extracellular macromolecules such as plasmid DNA to instantaneously enter cells without cytotoxicity [11–15,29,30]. Cavitation energy created by the collapse of the bubble has been considered as a key mechanism in intracellular delivery. This technique has been applied for site-specific intracellular delivery of macromolecules both *in vitro* and *in vivo* [11,16].

Microbubble reagents such as Optison, which are generally used in ultrasound imaging, could be used as gene delivery carriers together with ultrasound [11,16]. Although the mean diameter of Optison particles is about 2.0–4.5 μm, they contain bubbles of up to 32 μm in diameter, so Optison is too large to reach peripheral tissues. Tsunoda et al. reported that some mice died immediately after the administration of Optison i.v. even without sonication due to lethal embolisms in vital organs [31]. The same problem has not been reported in human, but there is a possibility that Optison cannot pass through capillary vessels. Optison were developed as ultrasound imaging agent. Thus, they had not been optimized for ultrasound imaging of peripheral tissues and gene delivery tool. Moreover, adding molecules with useful functions such as targeting is difficult because Optison is composed of albumin. We resolved these issues by developing Bubble liposomes that are derived by a novel method from liposomes. Suspensions of Bubble liposomes were cloudier than PEG-liposomes due to entrapment of perfluoropropane gas. Although the mean diameter of Bubble liposomes was about 1 μm according to dynamic light scattering, the suspension also contained many bubbles in the submicron range. Contrast microscopy showed that most of the Bubble liposomes were less than 3 μm in diameter. Moreover, 500 μg of Bubble liposomes (in terms of lipid amount) injected into the tail veins of mice, did not cause any deaths (data not shown), indicating that these novel liposomes would be safe for use *in vivo*. We are presently investigating the structure of Bubble liposomes by transmission electron microscopy.

Here, we investigated the feasibility of novel Bubble liposomes for gene delivery after ultrasound exposure. We initially examined whether perfluoropropane gas was associated with the Bubble liposomes. Ultrasound imaging revealed that echo signals are enhanced with Bubble liposomes compared with PEG-liposomes. In addition, Bubble liposomes collapsed after exposure to ultrasound, suggesting that ultrasound-induced cavitation. We then attempted to transduce plasmid DNA into cells using this feature of Bubble liposomes. Luciferase activity was very high after Bubble liposomes were exposed to ultrasound and cytotoxicity was absent. We examined the efficiency of transgene expression during transfection with plasmid DNA encoding EGFP. More cells were EGFP-positive in the presence, than in the absence of Bubble liposomes. In addition, the Bubble liposomes could transduce plasmid DNA into various tumor cells, T cell lines and endothelial cells. In general, transducing plasmid DNA into lymphocytes with non-viral vectors is difficult. Therefore, the transduction of plasmid DNA using Bubble liposomes into Jurkat cells, which are derived from T cell lines, is remarkable. In this gene delivery system, it is thought that gene expression is transient. To maintain gene expression for long time, it is necessary to repeat injection. Fortunately, Bubble liposomes were made of PEG-liposomes which were very low immunogenic. Therefore, it is thought that we could repeat injection of Bubble liposomes without reducing the ability of gene delivery in vivo.

In vivo gene delivery with Bubble liposomes and ultrasound, Bubble liposomes could effectively transduce plasmid DNA into the femoral artery. And this transfection efficiency of Bubble liposomes was higher than that of conventional lipofection methods using Lipofectamine 2000. This result suggested that Bubble liposomes could quickly transduce plasmid DNA into the artery by cavitation even under the condition of short contact time between Bubble liposomes and the endothelial cells and the existence of blood stream and serum. It was thought that plasmid DNA was transduced into endothelial cells in femoral artery because it was physiologically difficult for plasmid DNA and Bubble liposomes to extravasate from normal artery. In this study, mixture of plasmid DNA and Bubble liposomes was injected and we succeeded to deliver plasmid DNA in specific area by local exposure of ultrasound. Thus, gene expression depended on the site of ultrasound exposure. It was suggested that this system could induce gene targeting to the site where was exposed with ultrasound. In the future, we would like to establish non-invasive and tissue specific gene delivery with Bubble liposomes after systemic injection.

In this study, all data were obtained by using mixture of Bubble liposomes and plasmid DNA. Although gene expression was observed with mixture of plasmid DNA and Bubble liposomes and ultrasound exposure in femoral artery injection, it is important to control the biodistribution of both Bubble liposomes and plasmid DNA in systemic injection. In short, it is necessary for this gene delivery system to deliver both plasmid DNA and Bubble liposome to the same space. In addition, plasmid DNA is easily degraded with DNase. Therefore, to improve these problems, we are attempting to prepare the plasmid DNA entrapping type or complex type of Bubble liposomes.

We prepared Bubble liposomes that contained submicron-sized bubbles using a novel method. These novel liposomes induced cavitation upon exposure to ultrasound, which resulted in plasmid DNA transduction into cells in vitro and in vivo. These results suggested that our Bubble liposomes will be useful tools for gene delivery as well as being a universal ultrasound imaging agent.

5. Conclusion

This is the first report about the use of liposomal bubbles for gene delivery. In this study, we showed that combination of bubble liposomes and ultrasound exposure could be an effective and novel gene delivery method in vitro and in vivo. In the future, it is expected that bubble liposomes might be utilized as non-invasive gene delivery tools.

Acknowledgements

We are grateful to Dr. Katsuro Tachibana (Department of Anatomy, School of Medicine, Fukuoka University) for technical

advice regarding the induction of cavitation with ultrasound, to Mr. Yasuhiro Kuwata, Mr. Yusuke Oda, Mr. Takayuki Shibasaki, Ms. Ikumi Shinohara, Mr, Eisuke Namai, Mr. Yuta Saito, Ms. Naoko Yamashita, Mr. Yosuke Suyama (Department of Biopharmaceutics, School of Pharmaceutical Sciences, Teikyo University) for excellent technical assistance, to Dr. Yoshio Nakano and Dr. Akinori Suginaka (NOF Corporation) for technical advice regarding the lipids and for providing them, to Mr. Yasuhiko Hayakawa, Mr. Takahiro Yamauchi and Mr. Kosho Suzuki (NEPA GENE CO., LTD.) for technical advice regarding ultrasound exposure.

This study was supported by an Industrial Technology Research Grant (04A05010) in 2004 from the New Energy and Industrial Technology Development Organization (NEDO) of Japan and a Grant-in-Aid for the Encouragement of Young Scientists (160700392) and the Exploratory Research (16650126) from the Japan Society for the Promotion of Science.

References

[1] E. Check, Safety panel backs principle of gene-therapy trials, Nature 420 (2002) 595.
[2] E. Check, Second cancer case halts gene-therapy trials, Nature 421 (2003) 305.
[3] E. Marshall, Gene therapy death prompts review of adenovirus vector, Science 286 (1999) 2244–2245.
[4] C.C. Conwell, L. Huang, Recent progress in non-viral gene delivery, Non-viral Gene Therapy, Gene Design and Delivery, 2005, pp. 3–10.
[5] K. Wada, H. Arima, T. Tsutsumi, Y. Chihara, K. Hattori, F. Hirayama, K. Uekama, Improvement of gene delivery mediated by mannosylated dendrimer/alpha-cyclodextrin conjugates, J. Control. Release 104 (2005) 397–413.
[6] K. Kogure, R. Moriguchi, K. Sasaki, M. Ueno, S. Futaki, H. Harashima, Development of a non-viral multifunctional envelope-type nano device by a novel lipid film hydration method, J. Control. Release 98 (2004) 317–323.
[7] R. Moriguchi, K. Kogure, H. Akita, S. Futaki, M. Miyagishi, K. Taira, H. Harashima, A multifunctional envelope-type nano device for novel gene delivery of siRNA plasmids, Int. J. Pharm. 301 (2005) 277–285.
[8] H. Mizuguchi, T. Nakagawa, M. Nakanishi, S. Imazu, S. Nakagawa, T. Mayumi, Efficient gene transfer into mammalian cells using fusogenic liposome, Biochem. Biophys. Res. Commun. 218 (1996) 402–407.
[9] M. Fechheimer, J.F. Boylan, S. Parker, J.E. Sisken, G.L. Patel, S.G. Zimmer, Transfection of mammalian cells with plasmid DNA by scrape loading and sonication loading, Proc. Natl. Acad. Sci. U. S. A. 84 (1987) 8463–8467.
[10] W.J. Greenleaf, M.E. Bolander, G. Sarkar, M.B. Goldring, J.F. Greenleaf, Artificial cavitation nuclei significantly enhance acoustically induced cell transfection, Ultrasound Med. Biol. 24 (1998) 587–595.
[11] T. Li, K. Tachibana, M. Kuroki, M. Kuroki, Gene transfer with echo-enhanced contrast agents: comparison between Albunex, Optison, and Levovist in mice — initial results, Radiology 229 (2003) 423–428.
[12] Y. Taniyama, K. Tachibana, K. Hiraoka, M. Aoki, S. Yamamoto, K. Matsumoto, T. Nakamura, T. Ogihara, Y. Kaneda, R. Morishita, Development of safe and efficient novel nonviral gene transfer using ultrasound: enhancement of transfection efficiency of naked plasmid DNA in skeletal muscle, Gene Ther. 9 (2002) 372–380.
[13] Y. Taniyama, K. Tachibana, K. Hiraoka, T. Namba, K. Yamasaki, N. Hashiya, M. Aoki, T. Ogihara, K. Yasufumi, R. Morishita, Local delivery of plasmid DNA into rat carotid artery using ultrasound, Circulation 105 (2002) 1233–1239.
[14] S. Sonoda, K. Tachibana, E. Uchino, A. Okubo, M. Yamamoto, K. Sakoda, T. Hisatomi, K.H. Sonoda, Y. Negishi, Y. Izumi, S. Takao, T. Sakamoto, Gene transfer to corneal epithelium and keratocytes mediated by ultrasound with microbubbles, Investig. Ophthalmol. Vis. Sci. 47 (2006) 558–564.
[15] R.V. Shohet, S. Chen, Y.T. Zhou, Z. Wang, R.S. Meidell, R.H. Unger, P.A. Grayburn, Echocardiographic destruction of albumin microbubbles directs gene delivery to the myocardium, Circulation 101 (2000) 2554–2556.
[16] J.R. Lindner, Microbubbles in medical imaging: current applications and future directions, Nat. Rev. Drug. Discov. 3 (2004) 527–532.
[17] K. Kawamura, N. Kadowaki, R. Suzuki, S. Udagawa, S. Kasaoka, N. Utoguchi, T. Kitawaki, N. Sugimoto, N. Okada, K. Maruyama, T. Uchiyama, Dendritic cells that endocytosed antigen-containing IgG-liposomes elicit effective antitumor immunity, J. Immunother. 29 (2006) 165–174.
[18] H. Yanagie, K. Maruyama, T. Takizawa, O. Ishida, K. Ogura, T. Matsumoto, Y. Sakurai, T. Kobayashi, A. Shinohara, J. Rant, J. Skvarc, R. Ilic, G. Kuhne, M. Chiba, Y. Furuya, H. Sugiyama, T. Hisa, K. Ono, H. Kobayashi, M. Eriguchi, Application of boron-entrapped stealth liposomes to inhibition of growth of tumour cells in the in vivo boron neutron-capture therapy model, Biomed. Pharmacother. 60 (2006) 43–50.
[19] H. Yanagie, K. Ogura, K. Takagi, K. Maruyama, T. Matsumoto, Y. Sakurai, J. Skvarc, R. Illic, G. Kuhne, T. Hisa, I. Yoshizaki, K. Kono, Y. Furuya, H. Sugiyama, H. Kobayashi, K. Ono, K. Nakagawa, M. Eriguchi, Accumulation of boron compounds to tumor with polyethylene-glycol binding liposome by using neutron capture autoradiography, Appl. Radiat. Isotopes 61 (2004) 639–646.
[20] K. Maruyama, O. Ishida, S. Kasaoka, T. Takizawa, N. Utoguchi, A. Shinohara, M. Chiba, H. Kobayashi, M. Eriguchi, H. Yanagie, Intracellular targeting of sodium mercaptoundecahydrododecaborate (BSH) to solid tumors by transferrin-PEG liposomes, for boron neutron-capture therapy (BNCT), J. Control. Release 98 (2004) 195–207.
[21] M. Harata, Y. Soda, K. Tani, J. Ooi, T. Takizawa, M. Chen, Y. Bai, K. Izawa, S. Kobayashi, A. Tomonari, F. Nagamura, S. Takahashi, K. Uchimaru, T. Iseki, T. Tsuji, T.A. Takahashi, K. Sugita, S. Nakazawa, A. Tojo, K. Maruyama, S. Asano, CD19-targeting liposomes containing imatinib efficiently kill Philadelphia chromosome-positive acute lymphoblastic leukemia cells, Blood 104 (2004) 1442–1449.
[22] O. Ishida, K. Maruyama, H. Tanahashi, M. Iwatsuru, K. Sasaki, M. Eriguchi, H. Yanagie, Liposomes bearing polyethyleneglycol-coupled transferrin with intracellular targeting property to the solid tumors in vivo, Pharm. Res. 18 (2001) 1042–1048.
[23] K. Maruyama, E. Holmberg, S.J. Kennel, A. Klibanov, V.P. Torchilin, L. Huang, Characterization of in vivo immunoliposome targeting to pulmonary endothelium, J. Pharm. Sci. 79 (1990) 978–984.
[24] T. Mizoue, T. Horibe, K. Maruyama, T. Takizawa, M. Iwatsuru, K. Kono, H. Yanagie, F. Moriyasu, Targetability and intracellular delivery of anti-BCG antibody-modified, pH-sensitive fusogenic immunoliposomes to tumor cells, Int. J. Pharm. 237 (2002) 129–137.
[25] K. Maruyama, S.J. Kennel, L. Huang, Lipid composition is important for highly efficient target binding and retention of immunoliposomes, Proc. Natl. Acad. Sci. U. S. A. 87 (1990) 5744–5748.
[26] V. Mor-Avi, R.M. Lang, K.A. Robinson, C. Korcarz, A.F. Ng, P. Vignon, S. Akselrod, S.G. Shroff, Contrast echocardiographic quantification of regional myocardial perfusion: validation with an isolated rabbit heart model, J. Am. Soc. Echocardiogr. 9 (1996) 156–165.
[27] V. Mor-Avi, S.G. Shroff, K.A. Robinson, B.P. Cholley, A.F. Ng, R.M. Lang, Echocardiographic contrast agents and left ventricular contractility: evaluation using an isolated rabbit heart model, J. Am. Soc. Echocardiogr. 9 (1996) 452–461.
[28] T. Mosmann, Rapid colorimetric assay for cellular growth and survival: application to proliferation and cytotoxicity assays, J. Immunol. Methods 65 (1983) 55–63.
[29] M. Kinoshita, K. Hynynen, A novel method for the intracellular delivery of siRNA using microbubble-enhanced focused ultrasound, Biochem. Biophys. Res. Commun. 335 (2005) 393–399.
[30] M. Kinoshita, K. Hynynen, Intracellular delivery of Bak BH3 peptide by microbubble-enhanced ultrasound, Pharm. Res. 22 (2005) 716–720.
[31] S. Tsunoda, O. Mazda, Y. Oda, Y. Iida, S. Akabame, T. Kishida, M. Shin-Ya, H. Asada, S. Gojo, J. Imanishi, H. Matsubara, T. Yoshikawa, Sonoporation using microbubble BR14 promotes pDNA/siRNA transduction to murine heart, Biochem. Biophys. Res. Commun. 336 (2005) 118–127.

Development of the Liposomes Entrapped Ultrasound Imaging Gas ("Bubble Liposomes") as Novel Gene Delivery Carriers

Ryo Suzuki*, Kumiko Tanaka*, Kaori Sawamura*
Tomoko Takizawa*, Naoki Utoguchi*, Yoichi Negishi†
Kohsuke Hagisawa‡, Toshihiko Nishioka¶, Kazuo Maruyama*

*Department of Biopharmaceutics, School of Pharmaceutical Sciences, Teikyo University
1091-1 Suwarashi, Sagamiko, Tsukui, Kanagawa, 199-0195, Japan
†School of Pharmacy, Tokyo University of Pharmacy and Life Science
1432-1 Horinouchi, Hachioji, Tokyo, 192-0392, Japan
‡Department of Medical Engineering, National Defense Medical College
3-2 Namiki, Tokorozawa, 359-8513, Japan
¶Division of Cardiology, Saitama Medical Center, Saitama Medical School
1981 Tsujido, Kamoda, Kawagoe, 350-8550, Japan

Abstract. Recently, microbubbles and ultrasound have been investigated with a view to improving the transfection efficiency of nonviral delivery systems for gene by cavitation. However, microbubbles had some problems in terms of stability and targeting ability. To solve these problems, we paid attention to liposomes that had many advantages such as stable and safe *in vivo* and easy to modify targeting ligand. Previously, we have represented that liposomes are good drug and gene delivery carriers. In addition, we developed that the liposomes ("Bubble liposomes") were entrapped with perfluoropropane known as ultrasound imaging gas. In this study, we assessed about feasibility of "Bubble liposomes" as gene delivery tool utilized cavitation by ultrasound irradiation. "Bubble liposomes" could effectively deliver plasmid DNA to cells by combination of ultrasound irradiation without cyototoxicity. This result suggested that "Bubble liposomes" might be a new class of tool for gene delivery.

Keywords: Liposome, Gene delivery
PACS: 87.16.Dg, 87.54.Hk, 87.57.-s

INTRODUCTION

Gene therapy has a potentiality for treatment of cancer and diseases owning to genomic defects. It is important to select gene delivery vector which have good potency in terms of gene transduction efficiency, safe and easy to apply. In this situation, non-viral vectors are drawing the attention. However, they suffer from low transduction efficiencies. To improve this problem, many researchers attempt to develop effective gene delivery tool.

Recently, it was reported that microbubbles, which were contrast agents for medical ultrasound imaging, improved the transfection efficiency by cavitation with ultrasound

CP829, *Therapeutic Ultrasound: 5th International Symposium on Therapeutic Ultrasound*
edited by G. T. Clement, N. J. McDannold, and K. Hynynen

irradiation[1-3]. However, size of them is about 1-4 μm, it is too large to use for intravascular applications. It is necessary that they are held to a defined size, generally smaller than red blood cells and are sufficiently stable after injection into the blood. Additionally, it is known that microbubbles are difficult to modify on their surfaces such as addition of targeting function.

Previously, we developed the "Bubble liposomes" which were entrapped with perfluoropropane (PF) known as ultrasound imaging gas. The size of them was submicron, they could be used as intravascular application. In addition, it is easy to modify on liposome surface[4-7]. From the aspect of these, it is expected that "Bubble liposomes" might be a new type of bubble in medical field. Moreover, it is thought that cavitation would be induced by the ultrasound irradiation to "Bubble liposomes", and gene such as plasmid DNA could be delivered into cells. In this study, we assessed the feasibility of "Bubble liposomes" as gene delivery tool utilized cavitation by ultrasound irradiation.

CHARACTERISTICS OF "BUBBLE LIPOSOMES"

"Bubble liposomes" were made of conventional liposomes that were prepared with reverse phase evaporation method[8]. As shown Figure 1, "Bubble liposomes" became

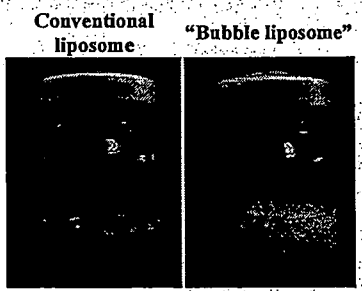

Figure 1. Appearance of conventional liposomes and " Bubble liposomes"

cloudy from conventional liposomes. This difference in appearance of these liposomes was thought to be related to PF gas entrapped within liposomes. To confirm the PF gas

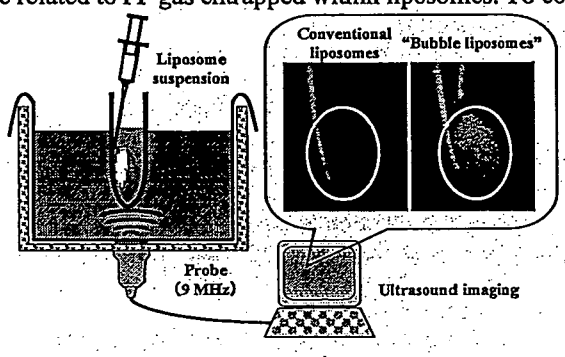

Figure 2. Ultrasound imaging of "Bubble liposomes"

within "Bubble liposome", they were imaged with a conventional ultrasound imaging machine (UF-750XT, Fukuda Denshi). Liposomes were injected into latex tube in water bath and imaged (Figure 2). "Bubble Liposomes" made ultrasound echo signal increased, but conventional liposomes did not so. Therefore, it confirmed that "Bubble liposomes" were including PF gas. In addition, it is expected that "Bubble liposomes" are able to be utilized as ultrasound imaging agents.

Next, we examined whether cavitation was induced with "Bubble liposomes" and ultrasound irradiation. Ultrasound irradiation was utilized with Sonoporation Gene Transfection System (SONOPORE, NEPA GENE CO., LTD.). The condition of ultrasound irradiation was shown Figure 3. When "Bubble liposomes" was irradiated

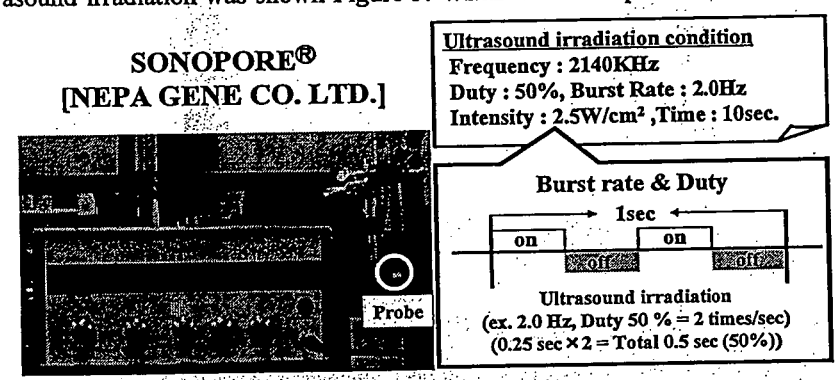

Figure 3. Condition of Ultrasound irradiation

with ultrasound, strength of ultrasound echo signal remarkably decreased with ultrasound imaging compared with ultrasound non-irradiated "Bubble liposomes" (Figure 4). This result suggested that cavitation was effectively induced by combination with "Bubble liposomes" and ultrasound irradiation. Therefore, it is thought that "Bubble liposomes" could be utilized as gene delivery carrier.

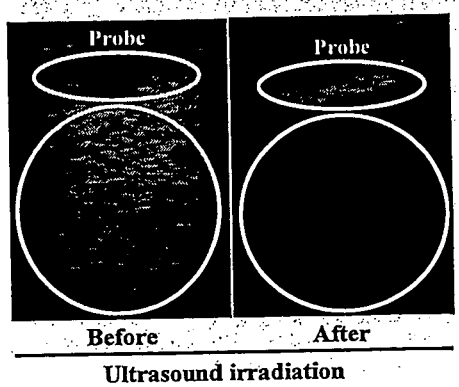

FIGURE 4. Ultrasound imaging of "Bubble liposomes" before and after ultrasound irradiation

"BUBBLE LIPOSOMES" AS GENE DELIVERY TOOL

Some researchers had reported about gene transfection utilized with microbubbles[2,3]. However, there was little of report about gene transfection with nano-bubbles. Thus, we examined about gene transfection with "Bubble liposomes" (FIGURE 5). When COS-7 cells were transfected with luciferase plasmid DNA

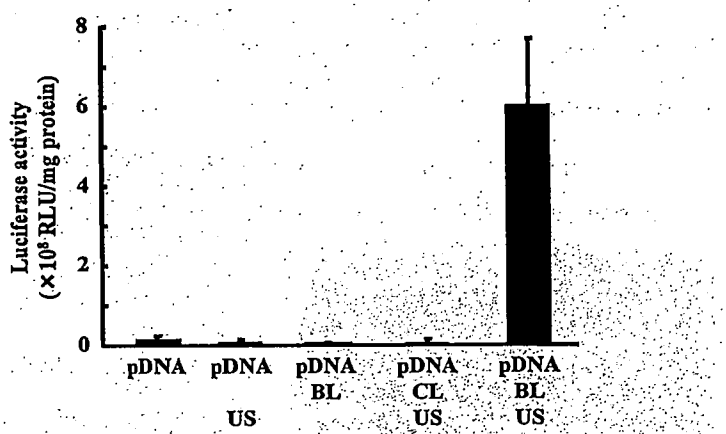

FIGURE 5. Gene transfection efficiency with "Bubble liposomes" and ultrasound irradiation

COS-7 cells were irradiated ultrasound with the condition as shown in FIGURE 3.
(BL: "Bubble liposomes", CL: Conventional liposomes, US: Ultrasound irradiation)

(pDNA) only or pDNA combined with ultrasound irradiation (general sonoporation), luciferase expression was not detectable. And it was also not detectable in the cells treated with mixture of pDNA and "Bubble liposomes" without ultrasound irradiation. In addition, pDNA was not transfected with conventional liposomes and ultrasound irradiation. On the other hand, combination of "Bubble liposomes" and ultrasound irradiation could effectively transfect pDNA into the cells due to induce the cavitation. Amazingly, the gene expression efficiency was very high with the ultrasound irradiation for 10 second though it was so short. Then, "Bubble liposomes" did not remarkably cytotoxicity (Data not shown). These results suggested that "Bubble liposomes" could be novel gene delivery carrier.

CONCLUSION

"Bubble liposomes" were imaged with ultrasound imaging machine. In addition, they could induce cavitation with ultrasound irradiation, and effectively and quickly introduce pDNA into the cells. Therefore, it was suggested that "Bubble liposomes" might be utilized as ultrasound imaging agent as well as gene delivery carrier.

ACKNOWLEDGMENTS

We are grateful to Dr. Katsuro Tachibana (Department of Anatomy, School of Medicine, Fukuoka University) for technical advice about cavitation induction with ultrasound irradiation, to Yasuhiro Kuwata, Ikumi Shinohara, Takayuki Shibasaki, Yusuke Oda, Shigeko Koyama and Mariko Tsukamoto (Department of Biopharmaceutics, School of Pharmaceutical Sciences, Teikyo University) for technical assistance, to Dr. Yoshio Nakano and Dr. Akinori Suginaka (NOF CORPORATION) for technical advice about lipids and providing them.

This study was supported by Industrial Technology Research Grand Program (04A05010) in '04 from New Energy and Industrial Technology Development Organization (NEDO) of Japan and Grant-in-Aid for the Encouragement of Young Scientists (160700392) from the Japan Society for the Promotion of Science.

REFERENCES

1. W.J. Greenleaf, M.E. Bolander, G. Sarkar, M.B. Goldring and J.F. Greenleaf, *Ultrasound Med. Biol.*, **24**, 587-595, (1998)
2. T. Li, K. Tachibana, M. Kuroki and M. Kuroki, *Radiology*, **229**: 423-428 (2003)
3. N. Hashiya, M. Aoki, K. Tachibana, Y. Taniyama, K. Yamasaki, K. Hiraoka, H. Makino, Y. Kaneda, T. Ogihara and R. Morishita, *Biochem. Biophys. Res. Commun.*, **317**, 508-514 (2004)
4. K. Maruyama, Liposomes, in *Non-virul Gene Therapy*, edited by K. Taira, K. Kataoka and T. Niidome, Springer-Verlag, Tokyo, 2005, pp. 19-35
5. M. Harata, Y. Soda, K. Tani, J. Ooi, T. Takizawa, M. Chen, Y. Bai, K. Izawa, S. Kobayashi, A. Tomonari, F. Nagamura, S. Takahashi, K. Uchimaru, T. Iseki, T. Tsuji, T.A. Takahashi, K. Sugita, S. Nakazawa, A. Tojo, K. Maruyama and S. Asano, *Blood*, **104**, 1442-1449 (2004)
6. K. Maruyama, O. Ishida, S. Kasaoka, T. Takizawa, N. Utoguchi, A. Shinohara, M. Chiba, H. Kobayashi, M. Eriguchi and H. Yanagie, *J. Control. Release*, **98**, 195-207 (2004)
7. K. Kawamura, N. Kadowaki, R. Suzuki, S. Udagawa, S. Kasaoka, N. Utoguchi, T. Kitawaki, N. Sugimoto, N. Okada, K. Maruyama and T. Uchiyama, *J. Immunotherapy.*, **in press**
8. F.J. Szoka and D. Papahadjopoulos, *Proc.Natl. Acad. Sci. U.S.A.*, **75**, 4194-4198 (1978)

VOLUME 117, NO. 2, 12 FEBRUARY 2007 ISSN: 0168-3659

ELSEVIER

journal of controlled release

OFFICIAL JOURNAL OF THE CONTROLLED RELEASE SOCIETY
AND THE JAPANESE SOCIETY OF DRUG DELIVERY SYSTEM